NASA TECHNICAL NOTE

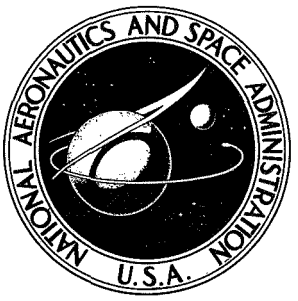

NASA TN D-6235

NASA TN D-6235

COMPARISON OF METHODS FOR IDENTIFYING PILOT DESCRIBING FUNCTIONS FROM CLOSED-LOOP OPERATING RECORDS

by Rodney C. Wingrove

Ames Research Center

Moffett Field, Calif. 94035

NATIONAL AERONAUTICS AND SPACE ADMINISTRATION • WASHINGTON, D. C. • MARCH 1971

1. Report No. NASA TN D-6235	2. Government Accession No.	3. Recipient's Catalog No.
4. Title and Subtitle COMPARISON OF METHODS FOR IDENTIFYING PILOT DESCRIBING FUNCTIONS FROM CLOSED-LOOP OPERATING RECORDS		5. Report Date March 1971 6. Performing Organization Code
7. Author(s) Rodney C. Wingrove		8. Performing Organization Report No. A-3578
9. Performing Organization Name and Address NASA Ames Research Center Moffett Field, Calif., 94035		10. Work Unit No. 125-19-01-16-00-21 11. Contract or Grant No.
12. Sponsoring Agency Name and Address National Aeronautics and Space Administration Washington, D. C., 20546		13. Type of Report and Period Covered Technical Note 14. Sponsoring Agency Code
15. Supplementary Notes		

16. Abstract

This report considers the problem of identifying the relationship between the pilot's input and output when he performs routing tracking tasks while controlling a system with dynamics approximating those of an airplane. A difficulty in using only the measured input and output data is that any extraneous output noise by the pilot is transferred through the control loop and results in an identification bias error. In this report three different identification methods are used to compare the amount of bias error. The three methods, which are the parameter model, orthogonal filters, and impulse-response techniques, are applied to the identification of both simulated (i.e., known) systems and piloted systems.

The identification of simulated systems illustrates that the amount of bias error depends upon the assumed system model. The bias error is reduced when the model used in the identification method has the same form (i.e., same number of coefficients, dynamic elements, etc.) as that of the simulated system. The parameter model method incorporates such a restricted model and consistently has the minimum bias error. The orthogonal filters and impulse-response methods allow, respectively, more general model forms and have more bias error.

The three identification methods are shown to estimate pilot describing functions adequately from representative tracking task data from both single-input and two-input control tasks with various levels of external disturbances. The results appear satisfactory even when the primary excitation comes from the pilot's own output noise.

17. Key Words (Suggested by Author(s))	18. Distribution Statement
Identification Pilot dynamics Closed-loop dynamics Flight test data Pilot describing functions	Unclassified-Unlimited

19. Security Classif. (of this report)	20. Security Classif. (of this page)	21. No. of Pages	22. Price*
Unclassified	Unclassified	39	$3.00

*For sale by the National Technical Information Service, Springfield, Virginia 22151

TABLE OF CONTENTS

NOMENCLATURE

$a_1, a_2, a_3 \ldots$	coefficients (with parameter model)
$b_1, b_2, b_3 \ldots$	coefficients (with orthogonal filters)
$G(j\omega)$	pilot describing function
$g(\tau)$	impulse response function
$H(j\omega)$	controlled element describing function
$i(t)$	external disturbance
$n(t)$	internal noise (pilot remnant)
$R_{ii}(\tau)$	autocorrelation function of i(t)
$R_{nn}(\tau)$	autocorrelation function of n(t)
$r(t)$	system output
T	total run length, sec
t	time, sec
$x(t)$	error signal (input to pilot)
$y(t)$	controller deflection (output of pilot)
$\varepsilon(t)$	residual
Δt	digitizing increment, sec
λ	time shift used during analysis, sec
τ_m	memory time, sec
τ_n	noise correlation time, sec
τ_G	time delay of pilot, sec
$\tau_1, \tau_2, \tau_3 \ldots$	time constants with orthogonal filters, sec
$\Phi_{ix}(j\omega)$	cross-power spectrum of i(t) and x(t)
$\Phi_{iy}(j\omega)$	cross-power spectrum of i(t) and y(t)
$\Phi_{ir}(j\omega)$	cross-power spectrum of i(t) and r(t)

$\Phi_{i_2 r_2}(j\omega)$	cross-power spectrum of $i_2(t)$ and $r_2(t)$
$\Phi_{ii}(j\omega)$	power spectrum of $i(t)$
$\Phi_{i_2 i_2}(j\omega)$	power spectrum of $i_2(t)$
$\hat{(\ )}$	estimated value
$\overline{(\ )^2}$	variance, $\frac{1}{T}\int_0^T (\ )^2\, dt$
$(\ )_1$	inner loop
$(\ )_2$	outer loop

COMPARISON OF METHODS FOR IDENTIFYING PILOT DESCRIBING FUNCTIONS FROM CLOSED-LOOP OPERATING RECORDS

Rodney C. Wingrove

Ames Research Center

SUMMARY

This report considers the problem of identifying the relationship between the pilot's input and output when he performs routing tracking tasks while controlling a system with dynamics approximating those of an airplane. A difficulty in using only the measured input and output data is that any extraneous output noise by the pilot is transferred through the control loop and results in an identification bias error. In this report three different identification methods are used to compare the amount of bias error. The three methods, which are the parameter model, orthogonal filters, and impulse-response techniques, are applied to the identification of both simulated (i.e., known) systems and piloted systems.

The identification of simulated systems illustrates that the amount of bias error depends upon the assumed system model. The bias error is reduced when the model used in the identification method has the same form (i.e., same number of coefficients, dynamic elements, etc.) as that of the simulated system. The parameter model method incorporates such a restricted model and consistently has the minimum bias error. The orthogonal filters and impulse-response methods allow, respectively, more general model forms and have more bias error.

The three identification methods are shown to estimate pilot describing functions adequately from representative tracking task data from both single-input and two-input control tasks with various levels of external disturbances. The results appear satisfactory even when the primary excitation comes from the pilot's own output noise.

INTRODUCTION

The input-output response of a pilot must be regarded as random, nonlinear, and dependent on the task he is performing. Many previous studies have shown that this type of response can be represented appropriately with a quasilinear system modeled by a linear element (describing function) and a remnant term (output noise). The pilot describing functions usually have been identified from records obtained in ground-based simulators (ref. 1) and flight tests (ref. 2) wherein carefully controlled external forcing functions are used to excite the pilot-vehicle system. The pilot describing functions are measured by comparing the input and output signals of the pilot with the

known forcing function. This technique minimizes those errors in identification due to any correlation of the input signal with the pilot's noise. Reference 3 is a good review of this work and summarizes the measured pilot describing functions.

Most other methods (refs. 4-12) for measuring pilot describing functions depend on random disturbances (e.g., aerodynamic turbulence, propulsive disturbance) to excite the pilot-vehicle system. These methods compute the describing function of the pilot from only his input and output signals. However, there is a fundamental error in identification because the output noise of the pilot is transmitted through the control loop and correlates with the pilot's input and output signals, thereby causing a bias error in identification. Reference 4 has shown that this bias error will be small if the amplitude of the pilot's noise is small compared with the amplitude of the other random disturbances in the control loop.

During routine flight-test operations, there are no carefully controlled forcing functions and even the random external disturbance may be quite small so that the principal system excitation may come from the pilot's output noise. Reference 5 has shown that, in this situation, it still may be possible, under certain conditions, to determine the pilot describing function without incurring an unacceptable identification error. Reference 5 showed that when the computer processing is constrained to identify only physically realizable describing functions, the identification error can be reduced by shifting the input signal during the computer processing an amount approximately equal to the time delay of the pilot. The theory shows that the identification error can be made small, by the time shift procedure, if the correlation time of pilot's noise is small (i.e., near "white" noise) compared with the sum of all time delays through the control loop. A somewhat different approach in reference 6 indicated that if the form of the identification model (e.g., number of coefficients, dynamic elements) used in the computer processing were restricted to be the same as that of the actual pilot's describing function, then the identification bias error may also be reduced. The studies in references 5 and 6 have shown, in effect, that the identification error may be strongly affected by the constraints in the identification model.

This report compares the results obtained from three identification methods which differ in the constraints placed on the describing function model. The impulse response method (refs. 4, 5, 10, and 11) assumes only that the describing function is physically realizable (i.e., the impulse response is constrained to be zero for negative time, ref. 5). A more constrained model is obtained with the orthogonal filter method (refs. 7 and 9) which assumes, in addition, that the describing function can be represented by a finite series of orthogonal filters. The most constrained model is obtained with the parameter model method (refs. 6, 8, 12) which assumes that the describing function can be represented by one specified model form (a simple second-order model is used for the results in this report). These three methods will be applied with the time shift procedure used in reference 5.

This report first describes the three identification methods and applies them in the identification of both simulated and piloted systems. The identification of the known systems will be used to show the effect of the output noise (relative magnitude and spectrum) on the identification bias error. These results will be compared with the theory of reference 5 and will also be used to show how the constraints, incorporated within each method, affect the identification error. The identification of piloted systems will illustrate the application of these methods for representative single-input and multi-input tracking tasks.

IDENTIFICATION METHODS

Before outlining the three identification methods used in this report, we shall briefly discuss the piloted control system elements. Figure 1 presents a block diagram of the pilot in a representative compensatory tracking task trying to control his output $y(t)$ so that the input error signal $x(t)$ is kept near zero. Generally, the input-output characteristics of the pilot must be considered as complex, nonlinear, and time varying. However, for the purposes of modeling, it is common practice to assume that his characteristics can be represented by a quasilinear system (ref. 3). This mathematical model contains the linear element G and the noise source n. The element $G(j\omega)$, which is called the pilot describing function,[1] is the frequency response of a linear constant coefficient system to the input $x(t)$. The term $n(t)$ represents the difference between output of the pilot, $y(t)$, and the output of the describing function $G(j\omega)$ driven by $x(t)$. Thus, $n(t)$ accounts for remnant terms such as nonlinearities, time variations, and additive noise in the output of the pilot.

The controlled system is mathematically characterized by the constant linear element H and the noise source i. The time history $i(t)$ accounts for nonlinearities and time variations in the controlled element, time-varying commands, and all disturbances from aerodynamics, propulsion, etc., external to the pilot.

In this report, we shall use each of the three methods to compute from the records $x(t)$ and $y(t)$, an estimate $\hat{G}(j\omega)$ that represents the best linear relationship between $x(t)$ and $y(t)$. "Best" here means that the integral of the squared residual,

$$\overline{\varepsilon^2} = \frac{1}{T}\int_0^T \varepsilon^2(t)dt$$

[1]Technically, $G(j\omega)$ represents a random input describing function because random, rather than sinusoidal, signals are used here (see ref. 3). Also, to avoid additional notation, terms such as $G(j\omega)$ and $H(j\omega)$ will be used to represent both the transfer functions of linear systems and the describing functions of nonlinear systems.

is minimized over a given record length, where $\varepsilon(t)$ is the difference between the actual record $y(t)$ and the output of the system $\hat{G}(j\omega)$ excited by $x(t)$. The following discussion will briefly describe the formulation of the three methods for the identification of single-input single-output systems. The formulation for multi-input systems (e.g., two input, one output) along with the details of the computer programing is further described in appendix A.

Parameter Model

The parameter model method assumes a particular describing function model for the pilot dynamics and then solves for the parameter in that model. The model[2] used for the results in this report has the form

$$G(j\omega) = \frac{a_3 j\omega + a_4}{(j\omega)^2 + a_1 j\omega + a_2} e^{-\lambda j\omega} \tag{1}$$

Estimates of the parameters a_1, a_2, a_3, a_4 are determined, as shown in appendix A, by a quasilinearization technique. The time shift λ accounts for any pure time delay in $G(j\omega)$. A method for choosing an appropriate value for λ is illustrated in appendix B.

The parameter model method is restricted in that only a limited set of systems, which have the specified form of equation (1), can be adequately identified.

Orthogonal Filters

The orthogonal filter method is somewhat more general than the parameter model method. It assumes that the unknown system dynamics can be modeled by a series of transfer functions of the form

$$G(j\omega) = e^{-\lambda j\omega}\left[\frac{b_1}{\tau_1 j\omega+1} + \frac{b_2(\tau_1 j\omega-1)}{(\tau_1 j\omega+1)(\tau_2 j\omega+1)} + \frac{b_3(\tau_1 j\omega-1)(\tau_2 j\omega-1)}{(\tau_1 j\omega+1)(\tau_2 j\omega+1)(\tau_3 j\omega+1)}\cdots\right] \tag{2}$$

This series is commonly called a set of Kautz (or linearly independent) filters. Estimates of the parameters b_1, b_2, b_3,. . . etc., are determined, as shown in appendix A, by a multiregression technique. For the results in this report, the first five filters in the series were used. The values of the time constants τ_1, τ_2, . . . τ_5 were taken (following ref. 7) as 1, 0.5, 0.25, 0.125, 0.0625 sec, respectively.

---

[2]This model form appears to be reasonable for the results in this report; however, the best model form will depend somewhat on each particular situation.

Impulse Response

The impulse response method assumes a very general input-output relationship that can be represented by the form

$$G(j\omega) = e^{-\lambda j\omega} \int_0^{\tau_m} g(\tau) e^{-\tau j\omega} \, d\tau \qquad (3)$$

Here $g(\tau)$ is an impulse response function that is assumed to be zero for $\tau < 0$ (i.e., $g(\tau)$ is constrained to be a physically realizable system) and also zero for $\tau > \tau_m$ (i.e., a finite memory time τ_m). The estimates for the impulse response function, as described in appendix A, are calculated at discrete times, $g(0)$, $g(\Delta t)$, $g(2\Delta t)$, etc. For the results in this report, the estimates were made at 20 discrete points.

IDENTIFICATION OF A KNOWN SYSTEM

In order to illustrate the results to be expected from each method just discussed, we shall first consider an example where the pilot dynamics are simulated; that is, where the describing function to be identified is known. For this example, the elements G and H were[3]

$$G(j\omega) = \frac{40\ j\omega + 50}{(j\omega)^2 + 3.5\ j\omega + 25} e^{-\tau_G j\omega}$$

and

$$H(j\omega) = \frac{j\omega + 0.585}{j\omega \left[(j\omega)^2 + 0.592\ j\omega + 0.584 \right]}$$

The dynamics for this example were simulated on a digital computer. The output of a random noise program was appropriately filtered to obtain the desired spectrums for $n(t)$ and $i(t)$. The resulting records for $x(t)$ and $y(t)$ were used with the three methods, as described in appendix A, to determine the estimate, $\hat{G}(j\omega)$.

Figure 2 presents the computed magnitude $|\hat{G}(j\omega)|$ and phase angle $\measuredangle \hat{G}(j\omega)$ as functions of frequency. Also shown for comparison are the magnitude $|G(j\omega)|$ and phase angle $\measuredangle G(j\omega)$ of the actual system. Two cases were simulated in order to illustrate the effect of the excitation source on the identification error. In the first case, the system dynamics are excited by both the external noise source $i(t)$ and the internal noise source $n(t)$. In the second case, the dynamics are only excited by the internal noise source $n(t)$ and $i(t) = 0$.

[3]The dynamics of G and H were taken to be near those of the piloted system in the next example.

Figure 2(a) presents the results for the case in which the system is excited by both the internal noise source and the external noise source. This figure shows that with this moderate amount of external disturbance ($\overline{i}^2 = 0.5\ \overline{n}^2$) the estimated describing functions $\hat{G}(j\omega)$ are generally near the actual system describing function $G(j\omega)$. The estimate derived by the parameter model method provides a nearly perfect match with the actual system $G(j\omega)$. The estimates derived by the orthogonal filters and impulse-response methods show only small differences between $\hat{G}(j\omega)$ and $G(j\omega)$. These differences are probably due to modeling error (i.e., these methods cannot exactly match the actual system model), and, because there is a bias error, due to the feedback of $n(t)$ through the control loop. The effect of this bias error is discussed in more detail with the next case.

Figure 2(b) presents the results for the case in which the system is excited by the internal noise source $n(t)$ and there is no external disturbance, $i(t) = 0$. This figure shows that with only an internal excitation, $\hat{G}(j\omega)$ may be quite different from $G(j\omega)$. This difference, or "identification bias error," is due to (ref. 5) the noise $n(t)$ being transmitted through the control loop producing a correlation between $n(t)$ and $x(t)$, so that the estimate tends to measure the negative inverse of the alternate path, $-1/H$, rather than measure the actual system G. The identification bias error is most clearly seen for the measured magnitude shown on the top of figure 2(b). The estimates $|\hat{G}(j\omega)|$ generally tend away from the actual system $|G(j\omega)|$ toward the curve shown for $|1/H(j\omega)|$.

The analysis in reference 5 has shown that the amount of bias error depends upon the relationship between the correlation time, τ_n, of the noise and the time delay, τ_G, in the control loop. An analytical expression for this bias error can be written as

$$\hat{G}(j\omega) = \underbrace{G(j\omega)}_{\text{actual system}} + \underbrace{e^{-\tau_n/\tau_G}\left[G(j\omega) - \frac{1}{H}(j\omega)\right] e^{-\tau_G(j\omega)}}_{\text{bias error}} \tag{4}$$

The primary assumptions in formulating this expression (ref. 5) are; (1) $i(t) = 0$, (2) $\lambda = \tau_G$, (3) the estimate $\hat{G}(j\omega)$ is constrained to be physically realizable, and (4) $H(j\omega)$ is minimum phase.

The magnitude of the bias error is directly related to the constant factor $e^{-\tau_n/\tau_G}$. For the simulated examples shown in figure 2, both the correlation time τ_n of the noise and the time delay τ_G in the simulated system were taken as 0.2 second. In order to illustrate the effect of these two quantities on the identification error, several runs were made with other values of τ_n and τ_G. Figure 3(a) presents results for various values of τ_n with τ_G held constant at 0.2 sec. Figure 3(b) presents results for various values of τ_G with τ_n held constant at 0.2 sec. The estimated magnitude $|\hat{G}|$ is presented at one frequency, $\omega = 1$ rad/sec. These estimates from the three identification methods are shown in comparison with the theory (eq.(4)) and with the actual value for the system ($|G| = 8.4$ dB) at $\omega = 1$ rad/sec.

The relative effects of noise correlation time τ_n and the time delay τ_G are apparent in figure 3. Increases in the noise time constant τ_n are seen in figure 3(a), to increase the bias error. The error will only be negligible when τ_n is near zero, that is, when the noise spectrum is near "white." Increasing the time delay τ_G (fig. 3(b)) decreases the identification error. The trends in figures 3(a) and 3(b) follow the theoretical considerations that the identification error will be small when the noise time constant is small compared with the time delay through the control loop.

Figure 3 shows that the difference between $|\hat{G}|$ and $|G|$ depends strongly on the particular identification method. We can note that the parameter model method, in which the model has the same form as the actual system, has an estimate $|\hat{G}|$ which is consistently closest to $|G|$. The orthogonal filters and impulse-response methods which are, respectively, less constrained, have estimates $|\hat{G}|$ further from $|G|$. The curve for the theory (ref. 5) was derived for an estimate that is constrained only to being physically realizable. The most general identification method, impulse response, is seen to be near this theoretical boundary. (The impulse-response method does not match this curve exactly because of restricted memory time τ_m noted with eq. (3).)

The results in figure 3 show that the identification error is related to the inherent constraints in the identification model. The identification error will be reduced when the model allowed by the identification method is restricted to a form that is near that of the pilot dynamics. In many practical situations, however, the exact form of the pilot dynamics will be unknown. In such cases, the more general methods, such as orthogonal filters and impulse response can be used to gain insight and possibly help to decide on a reasonable form for the pilot dynamics. The following examples illustrate applications wherein the combined use of all three methods aid in identification.

IDENTIFICATION OF PILOTED TRACKING DATA

Recorded data from the simulation study described in reference 13 will be used to illustrate the identification of pilot describing functions. In this example, the pilot controls the longitudinal axis of a simulated jet transport aircraft. Two cases will be analyzed. The first case is a single-input tracking task wherein the pilot controls the pitch attitude of the aircraft. The second case is a two-input tracking task wherein the pilot controls both the pitch attitude and altitude deviations of the aircraft.

The results to be presented in this report represent the average values computed from 12 minutes of tracking data (for subject A in ref. 13). Whereever possible, a comparison will be made between the results computed for this paper, and the results computed from the same data in reference 13.

Single-Input Task

In a single-input compensatory tracking task the pilot was trying to control his manipulator output $y(t)$ so that the attitude error signal $x(t)$ (displayed on an oscilloscope) was kept near zero. The simulated aircraft dynamics H had the form

$$H(j\omega) = \frac{j\omega + 0.585}{j\omega\left[(j\omega)^2 + 0.592\ j\omega + 0.584\right]}$$

and $i(t)$ was a superposition of eight continuous sine waves (table 1) which gave a random-appearing signal.

Pilot describing functions computed from the experimental records are presented in figure 4. Curves are shown for the three computational methods in this report and for comparison, the results determined in reference 13 are also shown.

Reference 13 used the standard cross-spectral method. The cross-spectra $\Phi_{iy}(j\omega)$ and $\Phi_{ix}(j\omega)$ were computed at each frequency contained in $i(t)$ and the pilot describing function was determined by the ratio $\Phi_{iy}(j\omega)/\Phi_{ix}(j\omega)$. This method, in effect, correlates the input $x(t)$ and output $y(t)$ with the known forcing function $i(t)$ and thereby eliminates the bias error in identification. The cross-spectral measurements, shown in figure 4, were made for three separate run lengths of four minutes each. The cross-spectral ratios are seen to have significant scatter in phase angle at low frequencies. (See ref. 14 for a discussion of this measurement problem.) Except for this uncertainty at the lower frequencies, there is generally good agreement between the cross-spectral ratio $\Phi_{iy}(j\omega)/\Phi_{ix}(j\omega)$ and the estimates $\hat{G}(j\omega)$ determined by the three methods in this report.

The residual terms calculated by the three identification methods for this example have the following values:

	$\overline{\varepsilon^2}/\overline{y^2}$
Parameter model	0.145
Orthogonal filters	.146
Impulse response	.144

The residual terms, shown normalized with respect to $\overline{y^2}$, represent about 14-1/2 percent of the pilots output. It is interesting that the residual for the parameter model method is about the same as that for the other less restricted methods. As further discussed in appendix B, this good agreement indicates that there is negligible modeling error with the parameter model estimate. Because there is good agreement between the curves of $\hat{G}(j\omega)$ in figure 4, and also good agreement between the residual values, it appears that

the chosen form of parameter model satisfactorily represents the pilot describing function for this example.

One way of verifying the results for this example is to consider the response of the closed-loop system. Let us take, for convenience, the parameter model estimate from figure 4 for the pilot describing function

$$\hat{G}(j\omega) = \frac{49.2\ j\omega + 62.4}{(j\omega)^2 + 3.65\ j\omega + 28.4}\ e^{-0.2\ j\omega}$$

With this function we can then calculate the transfer function between the input signal $i(t)$ and the output state, $r(t)$, as $\hat{G}(j\omega)H(j\omega)/[1+\hat{G}(j\omega)H(j\omega)]$. This curve is compared in figure 5 with the measured cross-spectral ratio $\Phi_{ir}(j\omega)/\Phi_{ii}(j\omega)$. Within the scatter of these cross-spectral measurements, we can see good agreement between the calculated closed-loop response, using $\hat{G}(j\omega)$, and the ratio $\Phi_{ir}(j\omega)/\Phi_{ii}(j\omega)$.

Two-Input Task

Figure 6 illustrates the two-input single-output tracking task analyzed in this case. The pilot is to keep both the inputs $x_1(t)$ and $x_2(t)$ near zero by the use of the manipulator output $y(t)$. The simulated inner-loop element H_1 and the disturbance $i_1(t)$ are identical to those in the single-input task just considered. The simulated outer-loop element H_2 had the form

$$H_2(j\omega) = \frac{2.28}{j\omega(j\omega + 0.585)}$$

and the input disturbance $i_2(t)$ was a superposition of seven sine waves (table 2) at frequencies spaced between those of the eight sine wave frequencies in $i_1(t)$.

Estimates for the pilot describing functions that were computed from the experimental records are presented in figure 7. The estimates $\hat{G}_1(j\omega)$ of the pilot response to the inner-loop signal are presented in figure 7(a) and the estimates $\hat{G}_2(j\omega)$ of the pilot response to the outer-loop signal are presented in figure 7(b). These results represent the average values derived from twelve minutes of pilot tracking data (again, subject A in ref. 13).

In figure 7(a), the cross-spectral results from reference 13 are compared with the results computed for this report. Significant scatter can be seen in the cross-spectra results. Reference 13 points out that fundamental limitations restrict the accuracy of these cross-spectral measurements in multiloop tasks. The three methods discussed in this report are seen to agree generally with each other for frequencies up to about 4 rad/sec. The only major differences are in the estimated magnitude $|G_1(j\omega)|$ at the higher frequencies. Generally, in the mid-frequency region between 0.4 and 4 rad/sec, the magnitude determined by the three methods agrees with the cross-spectral measurements,

and, except for the scatter in the cross-spectral measurements of phase angle at the lower frequencies, agrees with the phase angle results.

The estimates made by the three methods in this report for the pilot describing function $G_2(j\omega)$ in the outer loop, figure 7(b), show good agreement. A measurement of G_2, which might allow comparison with these results, was not computed in reference 13. We can, however, check the validity of the results in figure 7(b) by considering the estimated dynamics of the closed-loop system. Let us take the parameter model estimates (from fig. 7) for the pilot describing functions

$$\hat{G}_1(j\omega) = \frac{14.9\ j\omega + 14.4}{(j\omega)^2 + 2.5\ j\omega + 12.1} e^{-0.2j\omega}$$

$$\hat{G}_2(j\omega) = \frac{6.3\ j\omega + 3.8}{(j\omega)^2 + 2.5\ j\omega + 12.1} e^{-0.2j\omega}$$

With these values, we can then calculate the estimated transfer function between the input signal $i_2(t)$ and the output state $r_2(t)$ as

$$\frac{\hat{G}_2(j\omega)H_1(j\omega)H_2(j\omega)}{1 + \hat{G}_1(j\omega)H_1(j\omega) + \hat{G}_2(j\omega)H_1(j\omega)H_2(j\omega)}$$

This curve is compared in figure 8(a) with the cross-spectral ratio $\Phi_{i_2r_2}(j\omega)/\Phi_{i_2i_2}(j\omega)$. Although there was some scatter in these cross-spectral measurements, we can see good agreement between the calculated closed-loop response, when $\hat{G}_1(j\omega)$ and $\hat{G}_2(j\omega)$ are used and the computed cross-spectral ratio.

Two external disturbances, $i_1(t)$ and $i_2(t)$ were used to excite the dynamics for the two-input tracking data discussed up to this point. We will next illustrate some identification results when the excitation $i_1(t)$ is removed. For this situation, which was also simulated in reference 13, estimates were made with the three identification methods of this report. The results for the orthogonal filters and impulse-response methods were found to agree well with the parameter model results. Again, for convenience, the following estimates derived by the parameter model method only are given

$$\hat{G}_1(j\omega) = \frac{12.5\ j\omega + 7.7}{(j\omega)^2 + 3.1\ j\omega + 10} e^{-0.2j\omega}$$

$$\hat{G}_2(j\omega) = \frac{5.05\ j\omega + 1.8}{(j\omega)^2 + 3.1\ j\omega + 10} e^{-0.2j\omega}$$

The total closed-loop response, calculated from these estimates, is compared in figure 8(b) with the corresponding cross-spectral ratio $\Phi_{i_2r_2}(j\omega)/\Phi_{i_2i_2}(j\omega)$.

This figure shows very good agreement between the calculated closed-loop response, when $G_1(j\omega)$ and $G_2(j\omega)$ are used, and the measured cross-spectral ratio. This figure indicates that the results are adequate when only an outer loop disturbance, $i_2(t)$, is used to excite the closed-loop dynamics.

The identification for a pilot control task is illustrated next for the case when there are no significant external disturbances, i_1 or i_2. This illustration is interesting because only his output noise is used for system excitation.

APPLICATION TO A PILOT TASK WITH NO EXTERNAL DISTURBANCE

This example uses recorded data from the simulation study described in reference 15. This simulation represents a formation flying task in which the pilot is trying to hold his aircraft in a constant position behind a lead aircraft. Visual cues were presented to the pilot through a closed-circuit television system, and motion cues were applied with the Ames six-degrees-of-freedom motion device. For this example, only the lateral-directional control task will be analyzed for which the aircraft frequency response can be approximated as

$$H_1(j\omega) \approx \frac{4.3(j\omega)^2 + 2.2\, j\omega + 6.5}{j\omega\left[(j\omega)^3 + 1.3(j\omega)^2 + 2\, j\omega + 2.1\right]}$$

$$H_2(j\omega) \approx \frac{0.56}{(j\omega)^2}$$

The function $H_1(j\omega)$ approximates the dynamics from the pilot's lateral stick deflection to the aircraft roll attitude. The function $H_2(j\omega)$ approximates the dynamics between roll attitude and the aircraft lateral position. In this simulation, there were no significant[4] external noise sources, $i_1(t)$ or $i_2(t)$, so that the primary excitation came from the pilot's output noise.

The estimation of two independent functions $G_1(j\omega)$ and $G_2(j\omega)$ presents a fundamental problem in this situation because when $i_2(t) = 0$, the two input signals $x_1(t)$ and $x_2(t)$ (roll angle and lateral position) are exactly correlated. Solutions with the general identification methods, orthogonal filters and impulse response, are not possible in this situation (i.e., the matrix to be inverted, eq. (A2), becomes singular). With the parameter model method, however, a solution is possible because the restricted parameters in the model

[4]There may have been a small disturbance from several sources (simulation noise, coupling from other axes, long-term drift, etc.); however, the amplitude of the disturbance was quite small compared with the pilot's output noise.

are still linearly independent (i.e., the matrix, eq. (A5), is not singular). The measurements made with the parameter model give the following results:

$$\hat{G}_1(j\omega) = \frac{3.2\ j\omega + 5.7}{(j\omega)^2 + 2.2\ j\omega + 13.8}\ e^{-0.2j\omega}$$

$$\hat{G}_2(j\omega) = \frac{4.3\ j\omega + 1.4}{(j\omega)^2 + 2.2\ j\omega + 13.8}\ e^{-0.2j\omega}$$

These results cannot be verified as done in the previous example because there are no external disturbance sources, $i_1(t)$ or $i_2(t)$, that would allow alternate cross-spectral measurements. It is possible, however, to gain some insight into the adequacy of these results from the calculated closed-loop transfer functions. These functions, calculated with the estimates $\hat{G}_1(j\omega)$ and $\hat{G}_2(j\omega)$, are presented in the upper portion of figure 9. The transfer functions for n to y, n to x_1 and n to x_2 are presented in figures 9(a), 9(b), and 9(c), respectively. The calculated closed-loop response, when $\hat{G}_1(j\omega)$ and $\hat{G}_2(j\omega)$ are used, shows amplitude peaks at frequencies of 0.5 and 1.75 rad/sec. These two well-defined peaks correspond to the long and short-period closed-loop response of the combined pilot/vehicle dynamics. One would expect, therefore, to see large amplitude oscillations at these two frequencies in the operating records.

Power spectra were calculated from the operating records $y(t)$, $x_1(t)$ and $x_2(t)$. These power spectra are shown in the lower portions of figures 9(a), (b), (c), respectively. We see that the shape of the power spectra generally follow the trends calculated by the closed-loop transfer functions. In particular, each shows peaks near the frequencies of 0.5 and 1.75 rad/sec. This comparison of the power spectrum with the predicted closed-loop response does show that these estimates for $\hat{G}_1(j\omega)$ and $\hat{G}_2(j\omega)$ to appear reasonable.

CONCLUDING REMARKS

This report has compared the use of three methods for the identification of pilot describing functions from closed-loop operating records. Each method has inherent constraints that restrict the form of the identified describing functions. The impulse response method identifies a general class of describing functions that are constrained to be physically realizable. The orthogonal filters method identifies a more restricted class which is constrained, in addition to the above, to represent a finite series of dynamic models. The parameter model method identifies a very restricted class of describing functions which are further constrained to represent only one specified form of dynamic model. In addition, all of these methods use a time shift that is approximately equal to the time delay of the pilot.

This report shows that the identification bias error due to the correlation of the pilot's output noise in the control loop is related to the constraints imposed by each identification method. The parameter model method

is constrained to a specific form of pilot model and consistently has the minimum bias error. The orthogonal filters and impulse response methods are respectively less restricted and have respectively more bias error. This report also shows that, indepependent of the method, the bias error will be negligible only when the correlation time of the pilot's output noise is small (i.e., near "white") in relation to the time delay of the pilot.

The three methods were shown to estimate adequately the pilot describing function for representative single-input and two-input tracking task data. The primary advantage of these methods (as compared with the standard cross-spectral method) is that they can identify the pilot dynamics from routine closed-loop operating tasks where the external disturbance may be small, that is, in situations where the principal excitation comes from the pilot's own output noise.

Ames Research Center
National Aeronautics and Space Administration
Moffett Field, Calif., 94035, Sept. 23, 1970

APPENDIX A

COMPUTER PROCESSING EQUATIONS

The computer processing equations used for the three identification methods in this report are generalized to include any system with several inputs $x_1(t)$, $x_2(t)$ . . . $x_\ell(t)$ . . . and with one output $y(t)$.

Assume that the input and output time histories have been digitized at a uniform series of discrete points $k\Delta t$, where Δt represents the digitized increment. For each of the following techniques the input data are shifted by an amount λ, where λ represents the time delay of the pilot. The shifted input data will be represented as $x_\ell'(k)$, where $x_\ell'(k) = x_\ell(k\Delta t - \lambda)$. This time shifting of the digitized data and the processing equations, described below, was programmed on a digital computer. The solutions for the impulse response and orthogonal filter methods used a multiple regression technique. The parameter model method used a quasilinearization technique.

MULTIPLE REGRESSION

This technique (ref. 4) minimizes the least squares function

$$\sum_{k=1}^{K} [y(k) - \hat{y}(k)]^2$$

where K is the total number of data points and $\hat{y}(k)$ is the estimated output represented by

$$\hat{y}(k) = \sum_{j=1}^{J} \hat{b}_j Z_j(k) \tag{A1}$$

The terms $Z_j(k)$ are the result of operating (as will be shown below) on the input data. With this formulation, the coefficient b_j can be estimated by the following matrix inversion:

$$\begin{bmatrix} \hat{b}_1 \\ \cdot \\ \cdot \\ \cdot \\ \hat{b}_J \end{bmatrix} = \begin{bmatrix} \sum_{k=1}^{K} Z_1^2(k) & \cdots & \sum_{k=1}^{K} Z_1(k)Z_J(k) \\ & \vdots & \\ \sum_{k=1}^{K} Z_J(k)Z_1(k) & \cdots & \sum_{k=1}^{K} Z_J^2(k) \end{bmatrix}^{-1} \begin{bmatrix} \sum_{k=1}^{K} Z_1(k)y(k) \\ \\ \\ \sum_{k=1}^{K} Z_J(k)y(k) \end{bmatrix} \qquad \text{(A2)}$$

This general computing technique, which involves the inversion of a J×J matrix, was used for the impulse response and orthogonal filters methods. These methods differed primarily in the form of the operators, Z_j, in each case.

Impulse Response

The operators for the impulse response method are a series of simple time delays that operate on the imputs:

$$Z_1(k) = x_1'(k)$$

$$Z_2(k) = x_1'(k-1)$$

$$Z_3(k) = x_1'(k-2)$$

$$\cdot$$
$$\cdot$$
$$\cdot$$

or, in general,

$$Z_j(k) = x_l'(k-m)$$

where $j = (l-1)M + m + 1$. These operators represent a series of M simple time delays ($m = 0, 1, 2 \ldots M-1$) operating on the inputs $x_1'(k), x_2'(k) \ldots$

$x'_{\ell}(k)$ . . . . With these operators, the coefficients resulting from the computer solutions (eq. (A2)) are discrete values of the impulse response function

$$\hat{g}_{\ell}(m) = \hat{b}_j$$

where again $j = (\ell-1)M + m + 1$. This time domain solution was transferred into the frequency domain by the following simple discrete form approximation for the Fourier transform.

$$\hat{G}_{\ell}(j\omega) = e^{-\lambda j\omega}\ \Delta t \sum_{m=0}^{M-1} \hat{g}_{\ell}(m) e^{-m\Delta t j\omega} \tag{A3}$$

Orthogonal Filters

The operators for the orthogonal filters method represent the output of a series of filters driven by the inputs:

$$Z_1(k) = \sum_{m=0}^{M-1} d_1(m) x'_1(k-m)$$

$$Z_2(k) = \sum_{m=0}^{M-1} d_2(m) x'_1(k-m)$$

$$Z_3(k) = \sum_{m=0}^{M-1} d_3(m) x'_1(k-m)$$

$$\vdots$$

or, in general,

$$Z_j(k) = \sum_{m=0}^{M-1} d_i(m) x'_{\ell}(k-m)$$

where $j = (\ell-1)I + i$ and the terms $d_1(m)$, $d_2(m)$ . . . $d_1(m)$ . . . are a set of I discrete impulse response functions representing the set of orthogonal filters shown with equation (2) in the main text of this report.

The coefficients resulting from the computer solution (eq. (A2)) are used to calculate the estimate for the system impulse response function

$$\hat{g}_{\ell}(m) = \sum_{i=1}^{I} \hat{b}_j d_i(m)$$

where $j = (\ell-1)I + i$. These time domain impulse response functions are transformed into the frequency domain by means of equation (A3).

QUASILINEARIZATION

The quasilinearization technique assumes that the pilot dynamics can be modeled by a set of constant-coefficient linear differential equations (plus the time shift λ already mentioned). If a second-order model is chosen, the equations can be written in the form

$$\begin{bmatrix} \dot{\hat{y}}(k) \\ \dot{w}(k) \end{bmatrix} = \begin{bmatrix} -a_1 & 1 \\ -a_2 & 0 \end{bmatrix} \begin{bmatrix} \hat{y}(k) \\ w(k) \end{bmatrix} + \begin{bmatrix} a_3 & a_5 & \cdots \\ a_4 & a_6 & \cdots \end{bmatrix} \begin{bmatrix} x_1'(k) \\ x_2'(k) \\ \vdots \\ \vdots \end{bmatrix} \tag{A4}$$

where $w(k)$ is a dummy variable and $\hat{y}(k)$ represents the estimated output of the pilot. In order to match the estimated output with the measured output (minimize $\sum_{k=1}^{K} [y(k)-\hat{y}(k)]^2$), an initial estimate is made for $a_1, a_2, a_3 \ldots$. The following iterative procedure (ref. 16) is then used successively to improve the estimate

$$\begin{bmatrix} \hat{a}_1 \\ \hat{a}_2 \\ \vdots \end{bmatrix}_{new} = \begin{bmatrix} \hat{a}_1 \\ \hat{a}_2 \\ \vdots \end{bmatrix}_{old} + \begin{bmatrix} \sum_{k=1}^{K} z_1^2(k) & \sum_{k=1}^{K} z_1(k)z_2(k) & \cdots \\ \sum_{k=1}^{K} z_2(k)z_1(k) & \sum_{k=1}^{K} z_2^2(k) & \cdots \\ \vdots & \vdots & \cdots \end{bmatrix}^{-1} \begin{bmatrix} \sum_{k=1}^{K} z_1(k)[y(k)-\hat{y}(k)] \\ \sum_{k=1}^{K} z_2(k)[y(k)-\hat{y}(k)] \\ \vdots \end{bmatrix} \tag{A5}$$

On each iteration the system differential equations (eq. (A4)) were solved to determine the estimated output $\hat{y}(k)$ and the method of reference 17 was used to determine $z_j(k)$, where $z_j(k)$ is the gradient function $\partial\hat{y}(k)/\partial a_j$.

For the results in this report, it was found that reasonable convergence (from satisfactory initial estimates) was obtained in about five iterations. The estimated parameters from this time domain solution can be directly related to a frequency domain representation through transfer functions of the form

$$\hat{G}_1(j\omega) = \frac{\hat{a}_3 j\omega + \hat{a}_4}{(j\omega)^2 + \hat{a}_1 j\omega + \hat{a}_2} e^{-\lambda j\omega}$$

$$\hat{G}_2(j\omega) = \frac{\hat{a}_5 j\omega + \hat{a}_6}{(j\omega)^2 + \hat{a}_1 j\omega + \hat{a}_2} e^{-\lambda j\omega}$$

.
.
.

APPENDIX B

SELECTION OF THE TIME SHIFT λ

The time shift λ used with the computer processing equations to account for any time delay τ_G may be approximately known in some situations (e.g., ref. 3); but, in general, it will be unknown and will depend on the particular piloting task. The purpose of this appendix is to illustrate some results from using several values of λ and to illustrate the rationale in selecting the values of λ used for the results presented in the body of the text.

Figures 10(a) and (b) show the effect of the time shift λ on the residual $\overline{\varepsilon}^2$ (normalized with respect to the output $\overline{y}^2$). Results for the single-input task are presented in figure 10(a) and for the two-input task, in figure 10(b). These figures illustrate that the parameter model method is more sensitive to λ. The orthogonal filters and impulse-response methods, which are less restricted, are less sensitive to λ.

With both the single-input and two-input tasks, the residual for the parameter model method shows a minimum value at $\lambda = 0.2$ sec. For this method, the value of the pilots time delay τ_G is one of the parameters that must be estimated. It is therefore reasonable to choose a value for $\hat{\tau}_G = 0.2$ sec.

The residual error for the orthogonal filter and impulse-response methods shows (fig. 10(a)) a minimum value at $\lambda = 0$. (This is to be expected because with $\lambda = 0$ there is significant correlation between $n(t)$ and $x(t)$; see ref. 5.) The residual is about the same for values of λ from 0.1 sec to 0.3 sec. It was found that the form of the estimate $\hat{G}(j\omega)$, such as shown in figure 4, also has no appreciable difference for this range of λ from 0.1 to 0.3 sec. Therefore, for these more general methods, the estimate $\hat{G}(j\omega)$ is relatively insensitive to the exact value used for λ.

A value of $\lambda = 0.2$ sec, which is $\hat{\tau}_G$ estimated by the parameter model method, was used for the results presented in the body of the text. Figure 10 shows that, near the time shift $\lambda = 0.2$ sec, all the methods have about the same residual ($\overline{\varepsilon}^2/\overline{y}^2 = 0.14$ to 0.15) representing about 14 to 15 percent of the output $\overline{y}^2$. It is interesting that the amount of residual for the parameter model method is about the same as the amount of residual for other, less restricted, methods. It appears, therefore, that there is a negligible modeling error and the form chosen for the parameter model is reasonable for the results in this report.

REFERENCES

1. McRuer, Duane; Graham, Dunstan; Krendel, Ezra; and Reisener, William, Jr.: Human Pilot Dynamics in Compensatory Systems. Tech. Report AFFDL TR-65-15, Wright Patterson Air Force Base, Ohio, July 1965.

2. Newell, Fred D.; and Pietrzak, Paul E.: In-Flight Measurement of Human Response Characteristics. J. Aircraft, vol. 5, no. 3, May-June 1968, pp. 277-284.

3. McRuer, Duane T.; and Jex, Henry R.: A Review of Quasi-Linear Pilot Models. IEEE Transactions on Human Factors in Electronics, vol. HFE-8, no. 3, Sept. 1967, pp. 231-249.

4. Elkind, Jerome I.: Further Studies of Multiple Regression Analysis of Human Pilot Dynamic Responses: A Comparison of Analysis Techniques and Evaluation of Time-Varying Measurements. ASD-TDR-63-618, March 1964.

5. Wingrove, Rodney C.; and Edwards, Frederick G.: A Technique for Identifying Pilot Describing Functions From Routine Flight-Test Records. NASA TN D-5127, 1969.

6. Donaldson, P. E. K.: Error Decorrelation Studies on a Human Operator Performing a Balancing Task. Med. Electron. Biol. Eng., vol. 2, Pergamon Press, 1964, pp. 393-410. Printed in Great Britain.

7. Elkind, Jerome I.; Starr, Edward A.; Green, David M.; and Darley, D. Lucille: Evaluation of a Technique for Determining Time-Invariant and Time-Variant Dynamic Characteristics of Human Pilots. NASA TN D-1897, 1963.

8. Todosiev, E. P.; Rose, R. E.; Bekey, G. A.; and Williams, H. L.: Human Tracking Performance in Uncoupled and Coupled Two-Axis Systems. NASA CR-532, 1966.

9. Wierwille, Walter W.; and Gagne, Gilbert A.: A Theory for the Optimal Deterministic Characterization of the Time-Varying Dynamics of the Human Operator. NASA CR-170, 1965.

10. Taylor, Lawrence W., Jr.: A Comparison of Human Response Modeling in the Time and Frequency Domains. 3rd Annual NASA-University Conference on Manual Control. NASA SP-144, 1967, pp. 137-153.

11. Goodman, T. P.; and Reswick, J. B.: Determination of System Characteristics from Normal Operating Records. Trans. ASME, vol. 78, no. 2, Feb. 1956, pp. 259-268.

12. Adams, James J.; Bergeron, Hugh P.; and Hurt, George J., Jr.: Human Transfer Functions in Multi-Axis and Multi-Loop Control Systems. NASA TN D-3305, 1966.

13. Stapleford, Robert L.; Craig, Samuel J.; and Tennant, Jean A.: Measurement of Pilot Describing Functions in Single-Controller Multiloop Tasks. NASA CR-1238, 1969.

14. Taylor, Lawrence W.: A Look at Pilot Modeling Techniques at Low Frequencies. Proc. Sixth Annual Conference on Manual Control, April 7-9, 1970, AFIT-AFFDL, Wright Patterson AFB, Ohio, pp. 871-896.

15. Schmidt, Stanley F.; and Conrad, Bjorn: Motion Drive Signals for Piloted Flight Simulators. NASA CR-1601, 1970.

16. Denery, Dallas G.: A Parameter Estimation Procedure Which is Insensitive to Initial Parameter Estimates. AIAA Paper 70-34, 1970.

17. Meissenger, Hans F.: The Use of Parameter Influence Coefficients in Computer Analysis of Dynamic Systems. Proc. Western Joint Computer Conference, May 1960.

TABLE 1.- THE EIGHT SINE WAVES SUPERIMPOSED TO REPRESENT THE SIGNALS $i(t)$ or $i_1(t)$

Frequency (rad/sec)	Relative magnitude
0.157	1
.288	1
.524	1
.969	1
1.75	0.1
3.25	.1
6.00	.1
11.1	.1

TABLE 2.- THE SEVEN SINE WAVES SUPERIMPOSED TO REPRESENT THE SIGNAL $i_2(t)$

Frequency (rad/sec)	Relative magnitude
0.209	1
.367	1
.681	1
1.28	0.1
2.38	.1
4.42	.1
8.17	.1

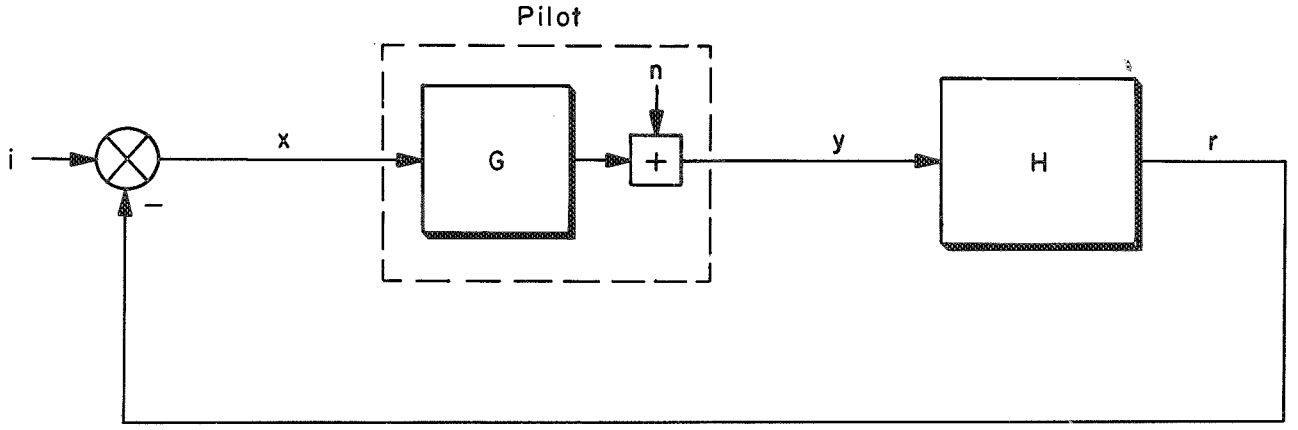

Figure 1.- The pilot and control system elements for a single-input, single-output task.

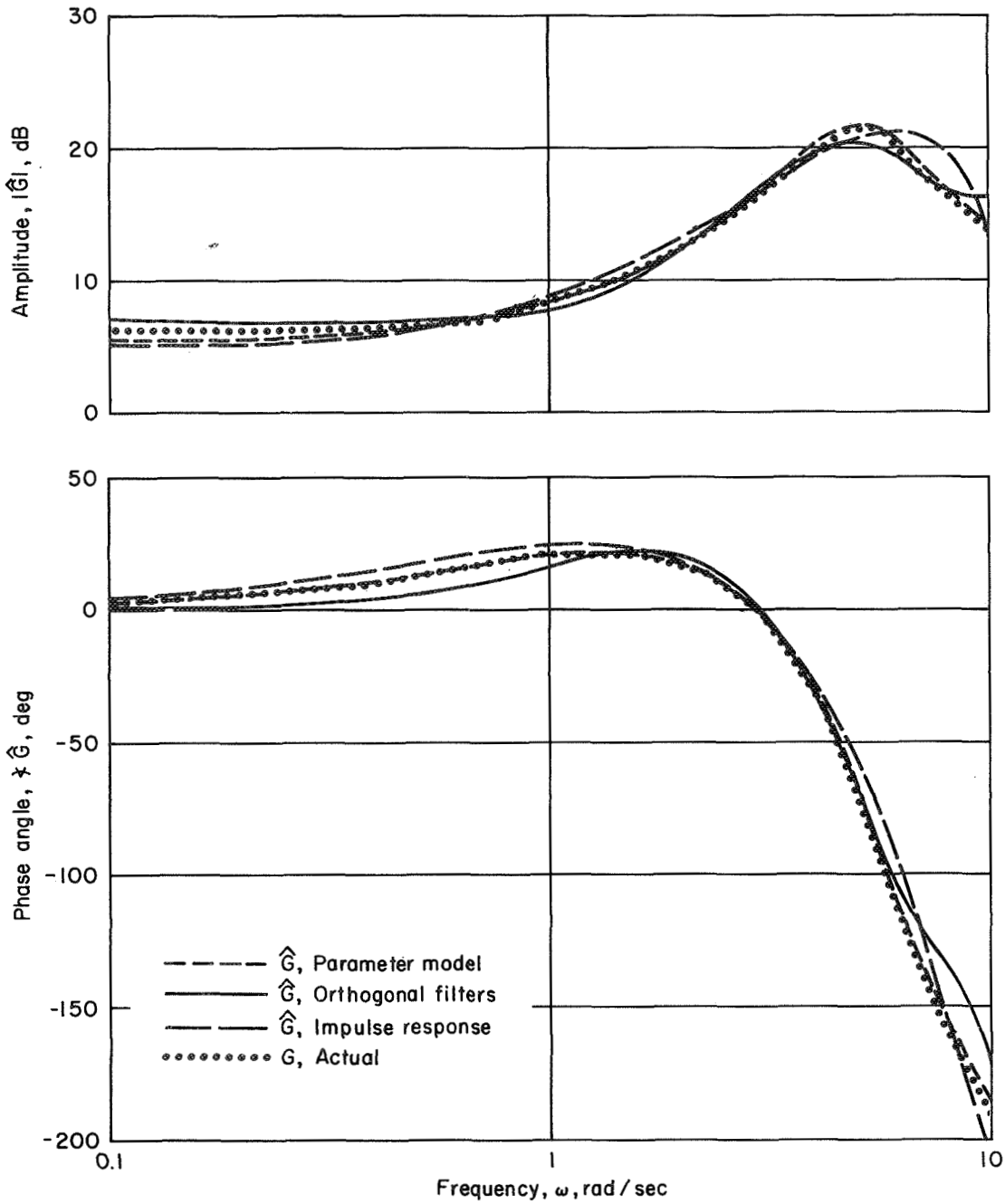

(a) With external disturbance; $R_{ii}(\tau) = 0.5e^{-|\tau|}$

Figure 2.- Identification of known system; $R_{nn}(\tau) = e^{-|\tau/0.2|}$, $\lambda = \tau_G = 0.2$

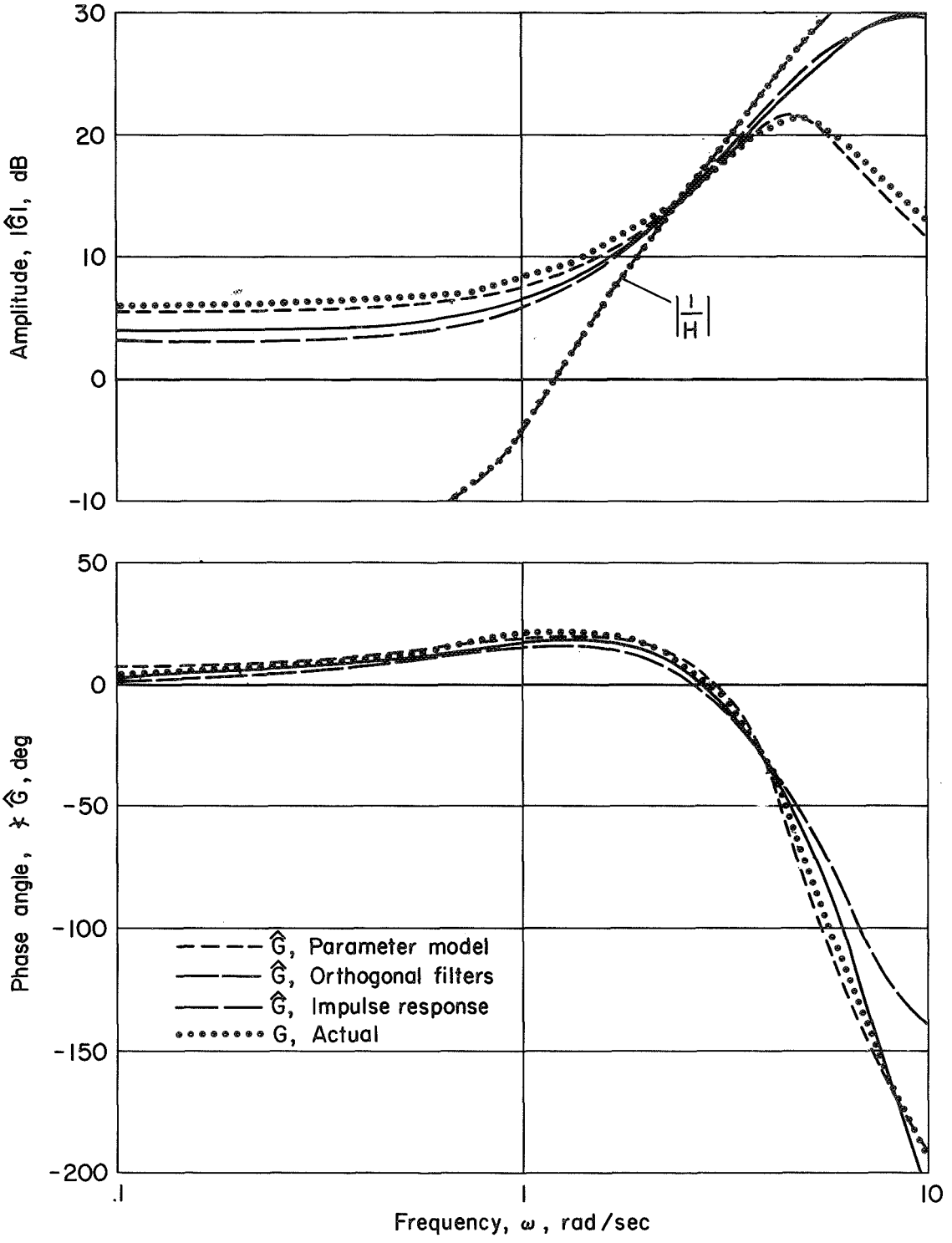

(b) No external disturbance; i = 0

Figure 2.- Concluded.

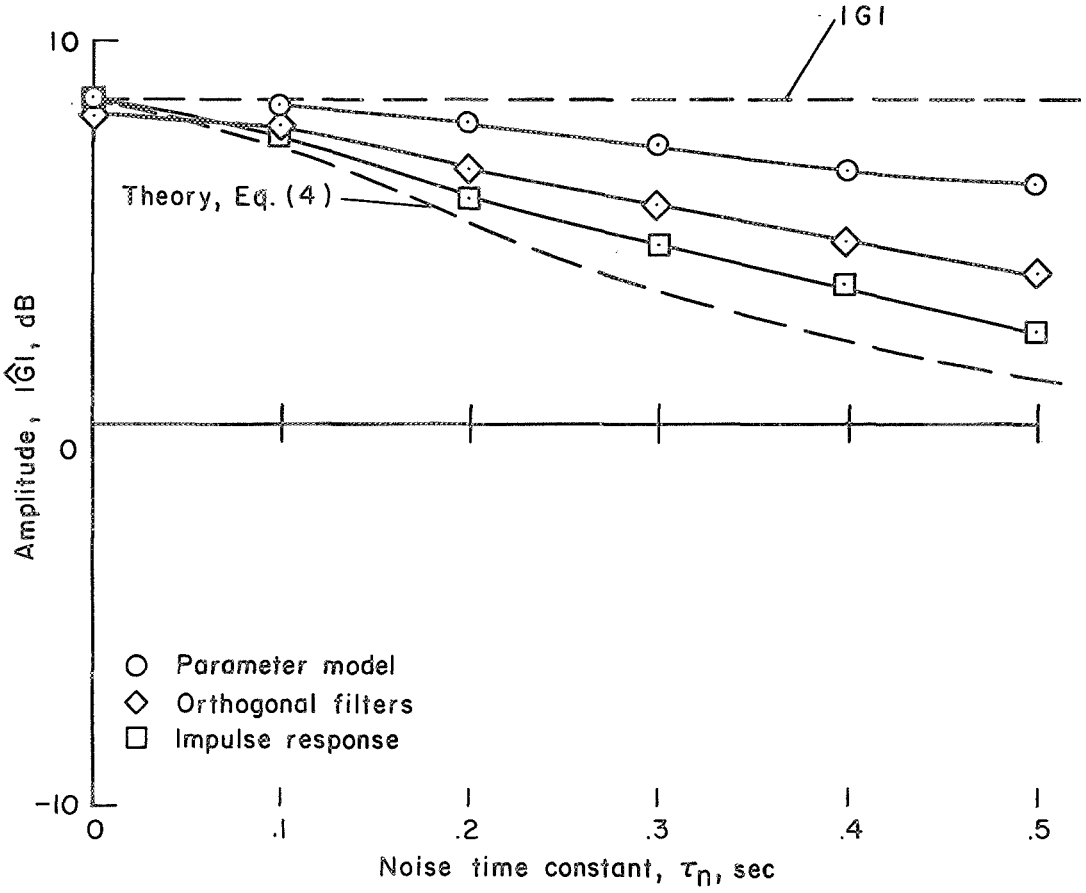

(a) Effect of τ_n; τ_G = 0.2 sec.

Figure 3.- Effect of τ_n and τ_G on the identification of a known system; i = 0, $R_{nn}(\tau) = e^{-|\tau/\tau_n|}$, $\lambda = \tau_G$, ω = 1 rad/sec.

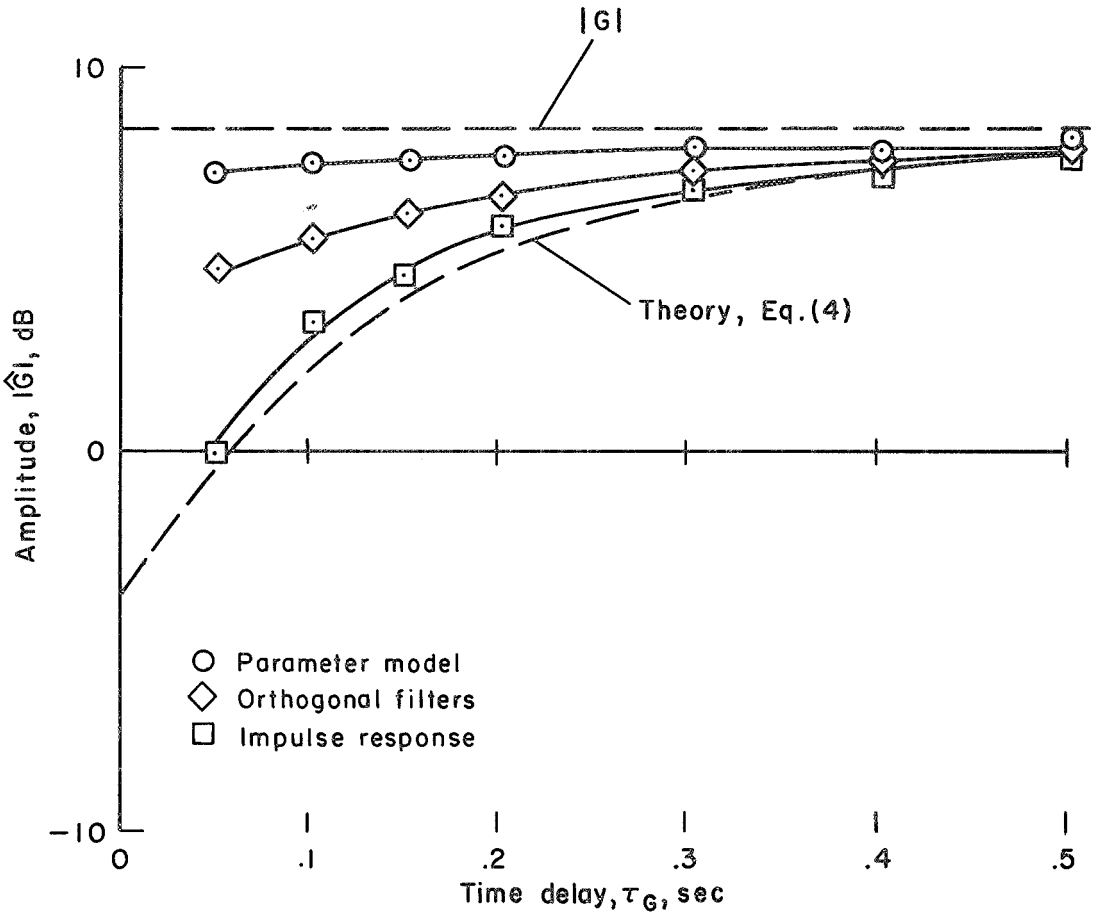

(b) Effect of τ_G; τ_n = 0.2 sec.

Figure 3.- Concluded.

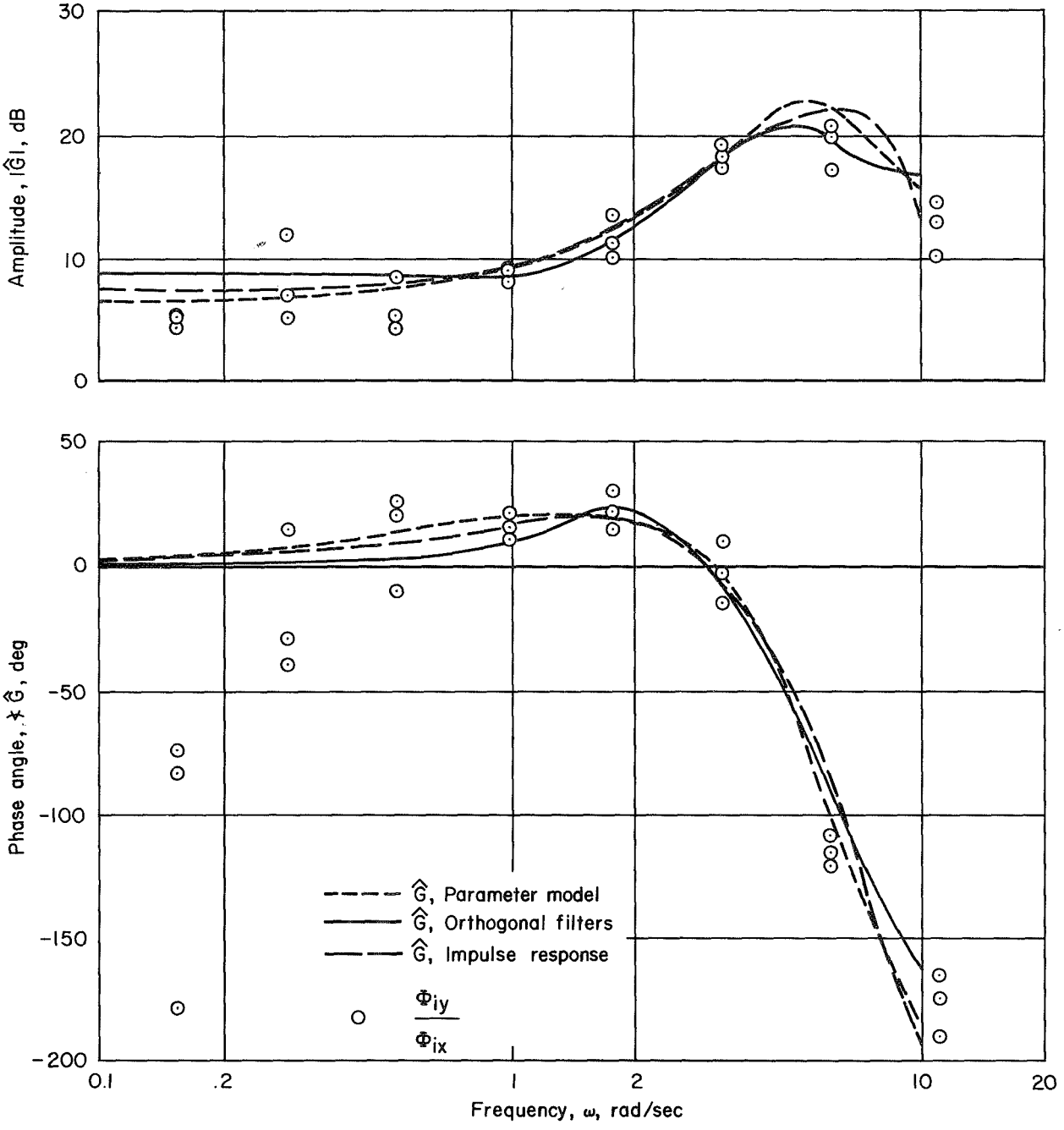

Figure 4.- Identification of piloted tracking data; single-input task, $\lambda = 0.2$ sec.

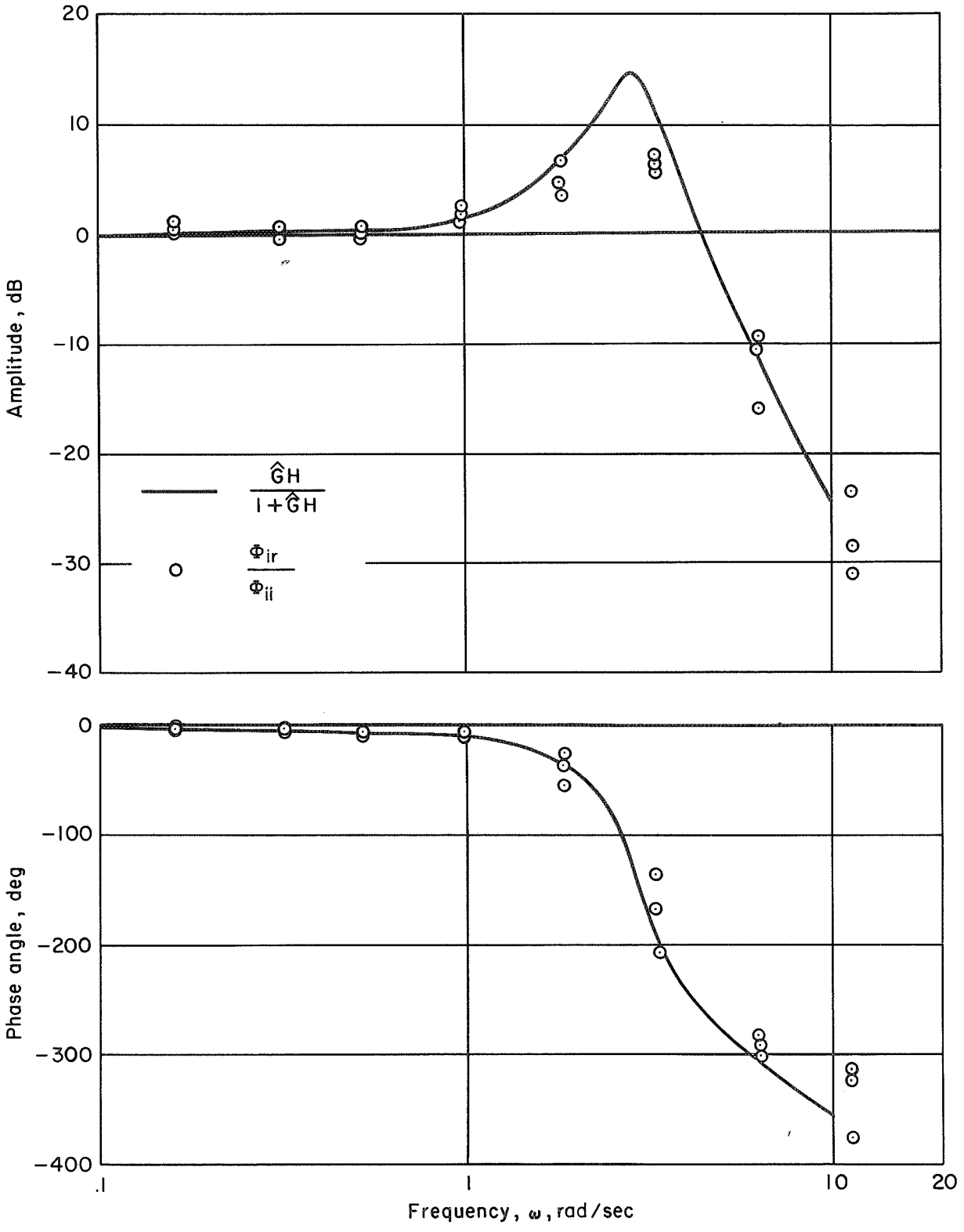

Figure 5.- Estimation of closed-loop dynamics; single-input task.

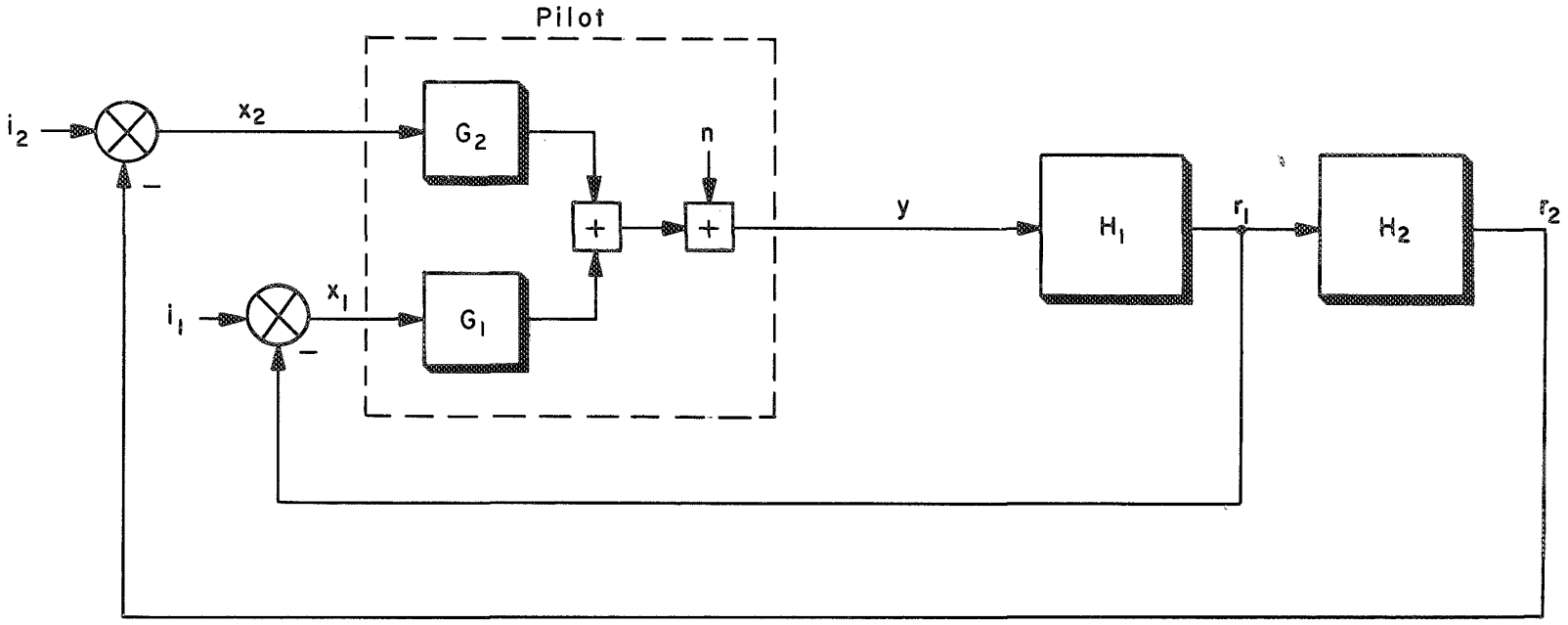

Figure 6.- The pilot and control system elements for a two-input single-output tracking task.

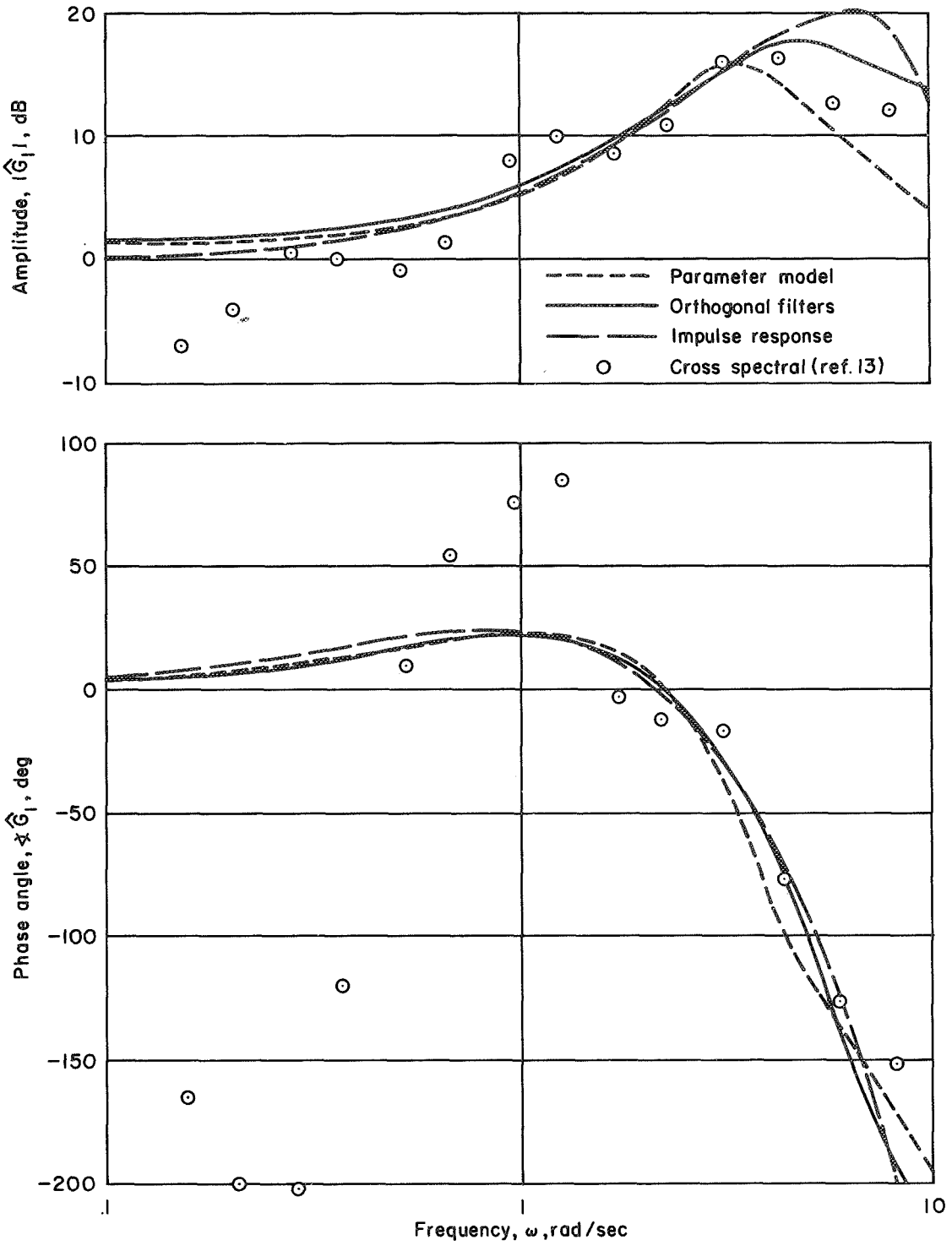

(a) Inner loop.

Figure 7.- Identification of piloted tracking data; two-input task $\lambda = 0.2$ sec.

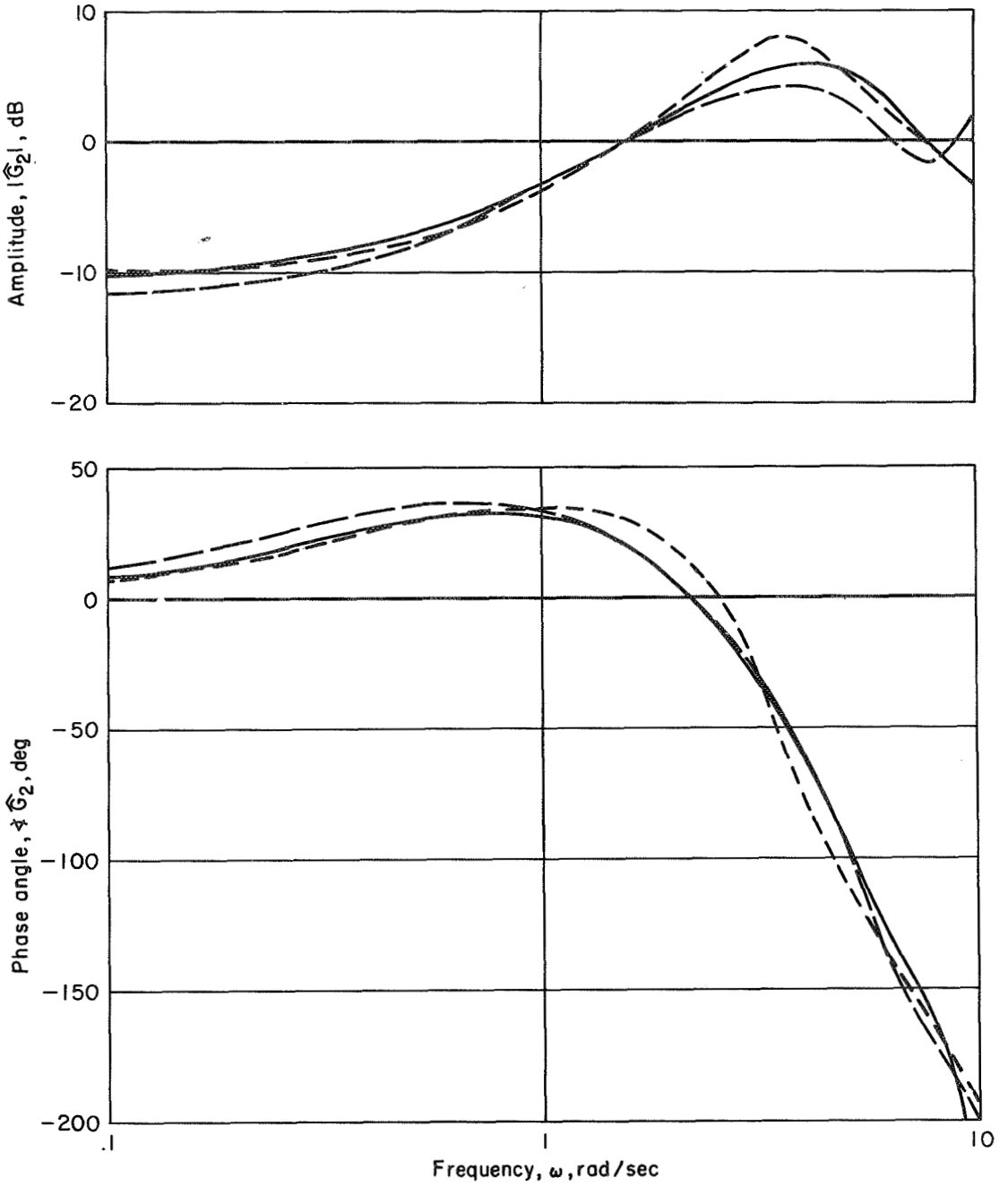

(b) Outer loop.

Figure 7.- Concluded.

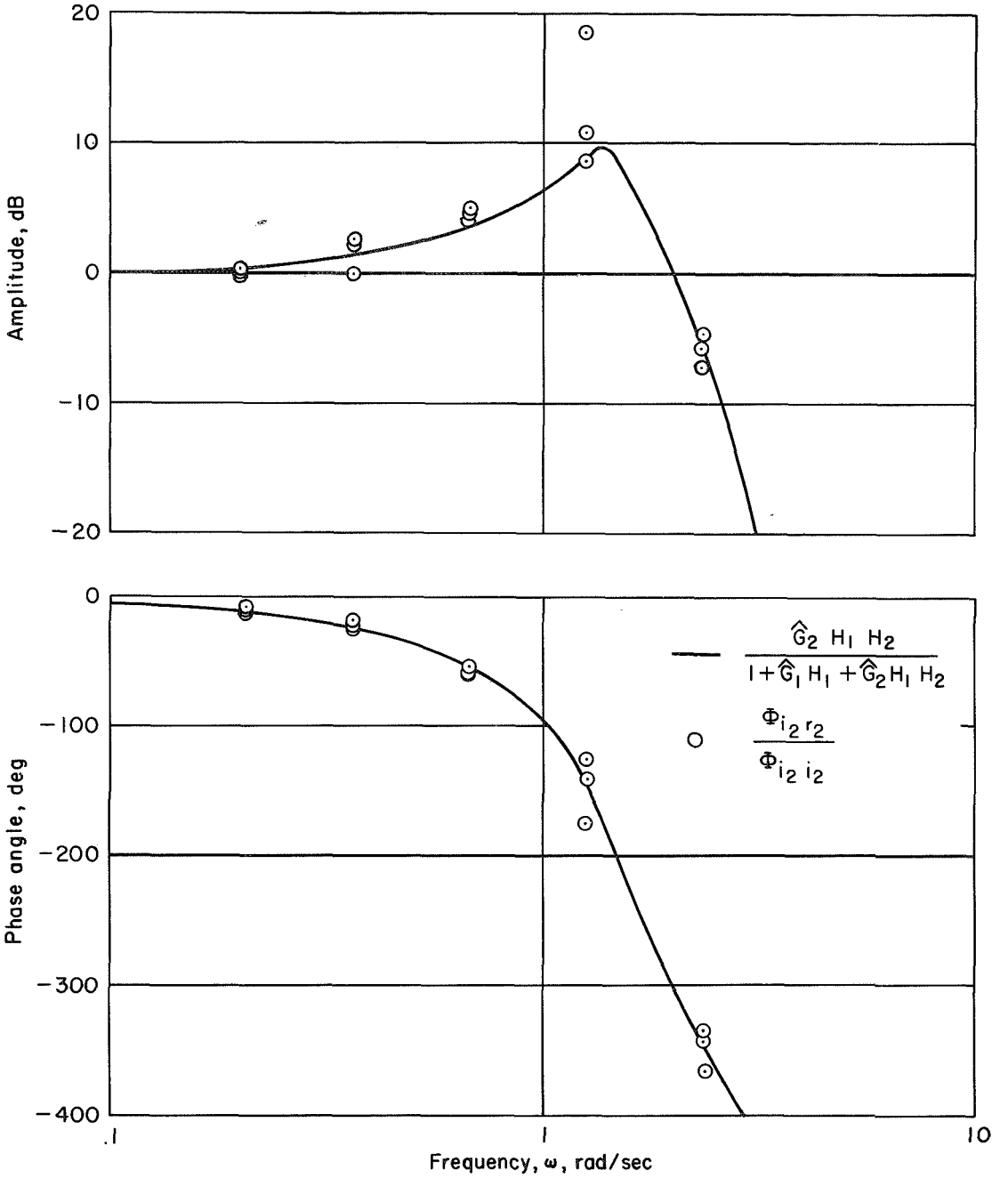

(a) Two external disturbances; i_1 and i_2.

Figure 8.- Estimation of closed-loop dynamics; two-input task.

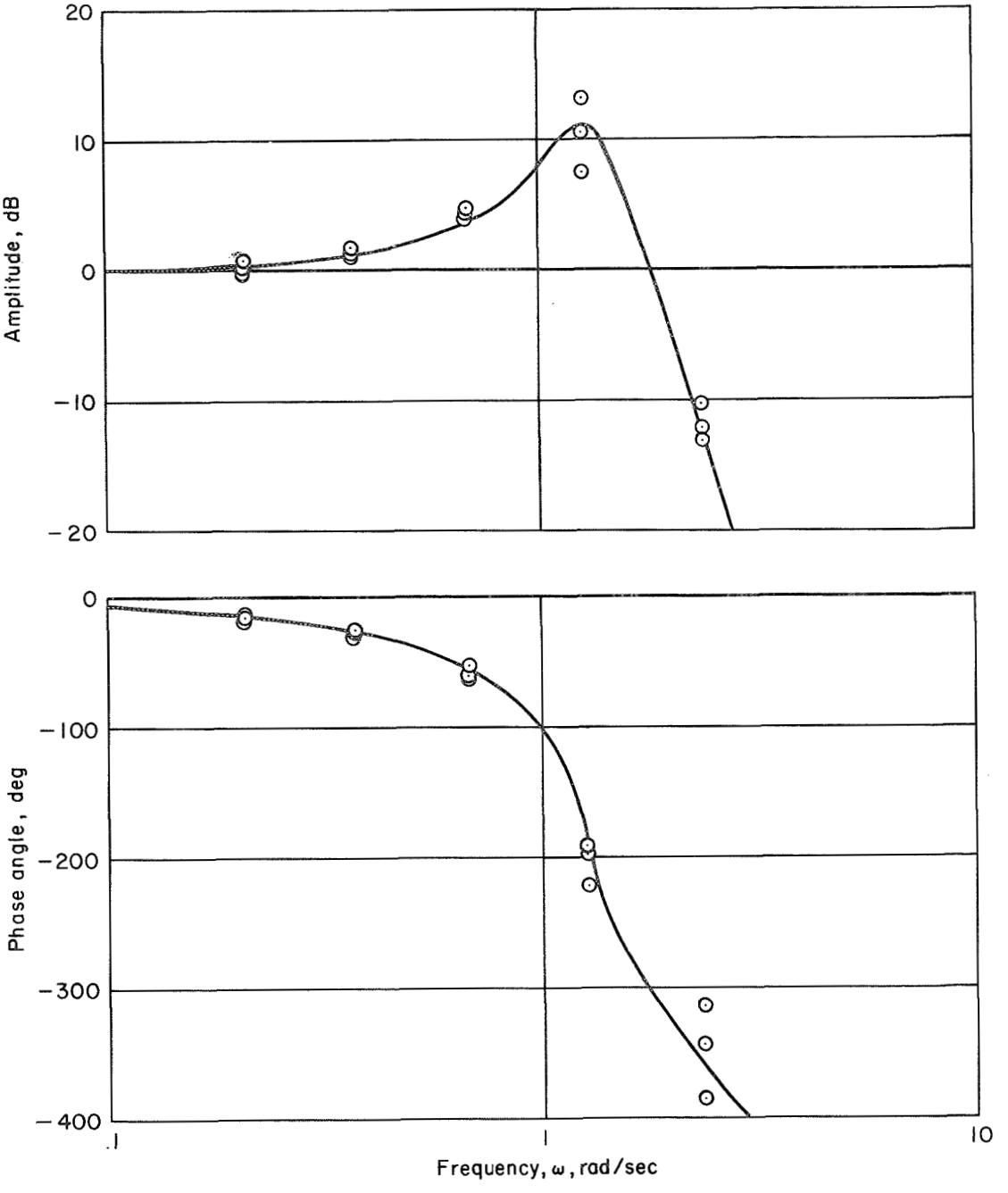

(b) One external disturbance i_2; $i_1 = 0$.

Figure 8.- Concluded.

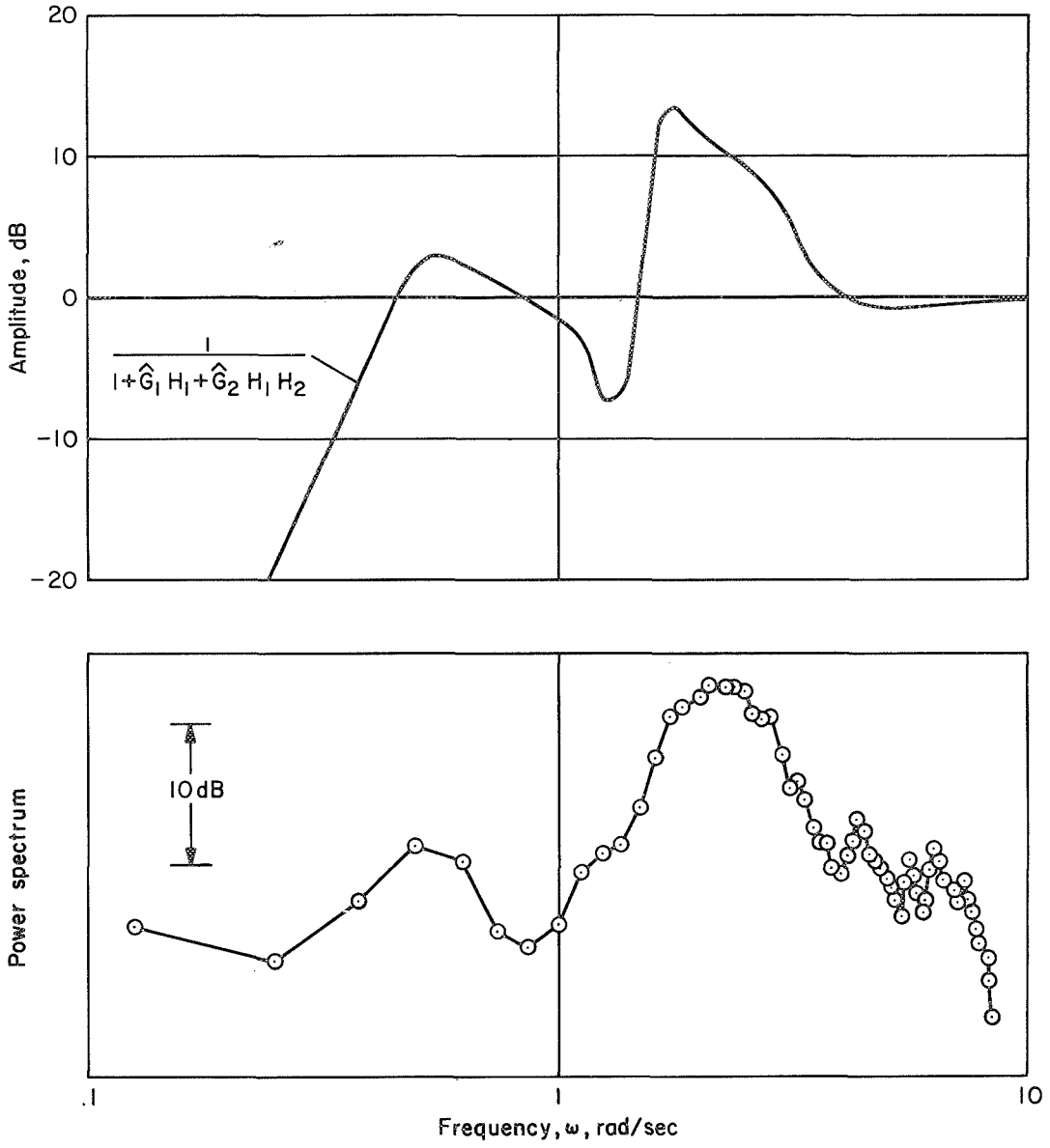

(a) The describing function n to y compared with the power spectrum of y(t).

Figure 9.- Calculated describing functions compared with measured power spectrums; two-input task with no external disturbance.

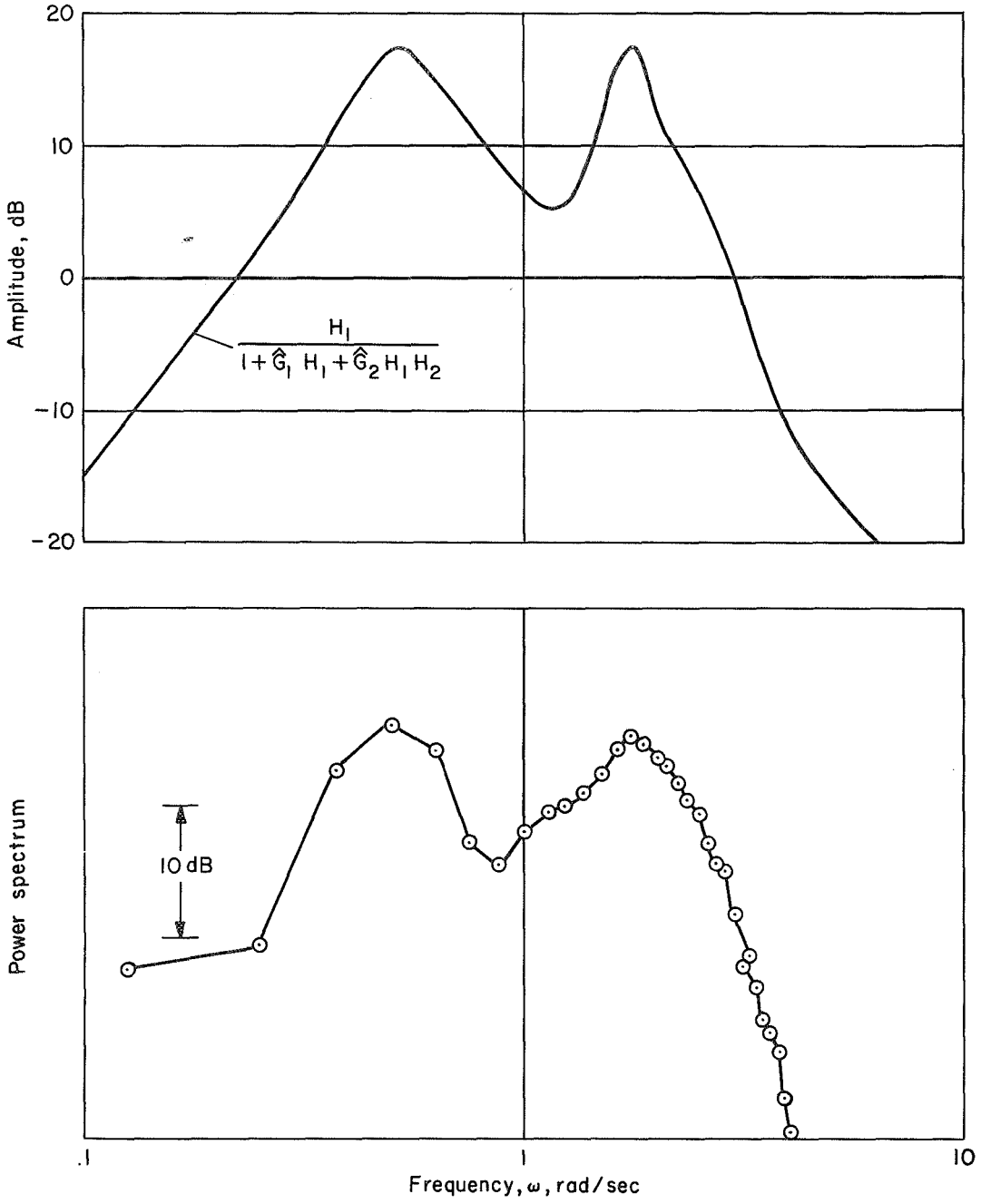

(b) The describing function n to x_1 compared with the power spectrum of $x_1(t)$.

Figure 9.- Continued.

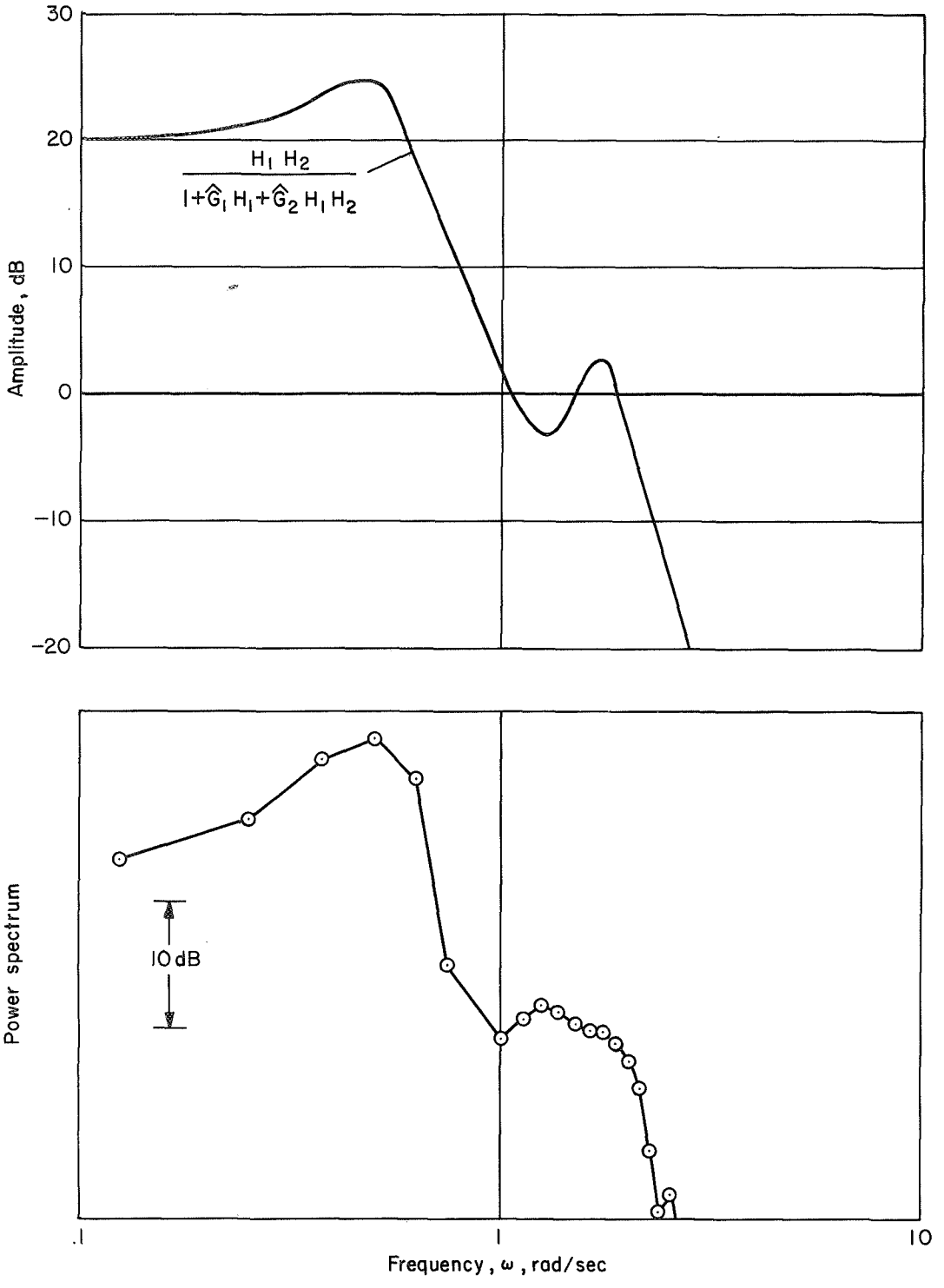

(c) The describing function n to x_2 compared with the power spectrum of $x_2(t)$.

Figure 9.- Concluded.

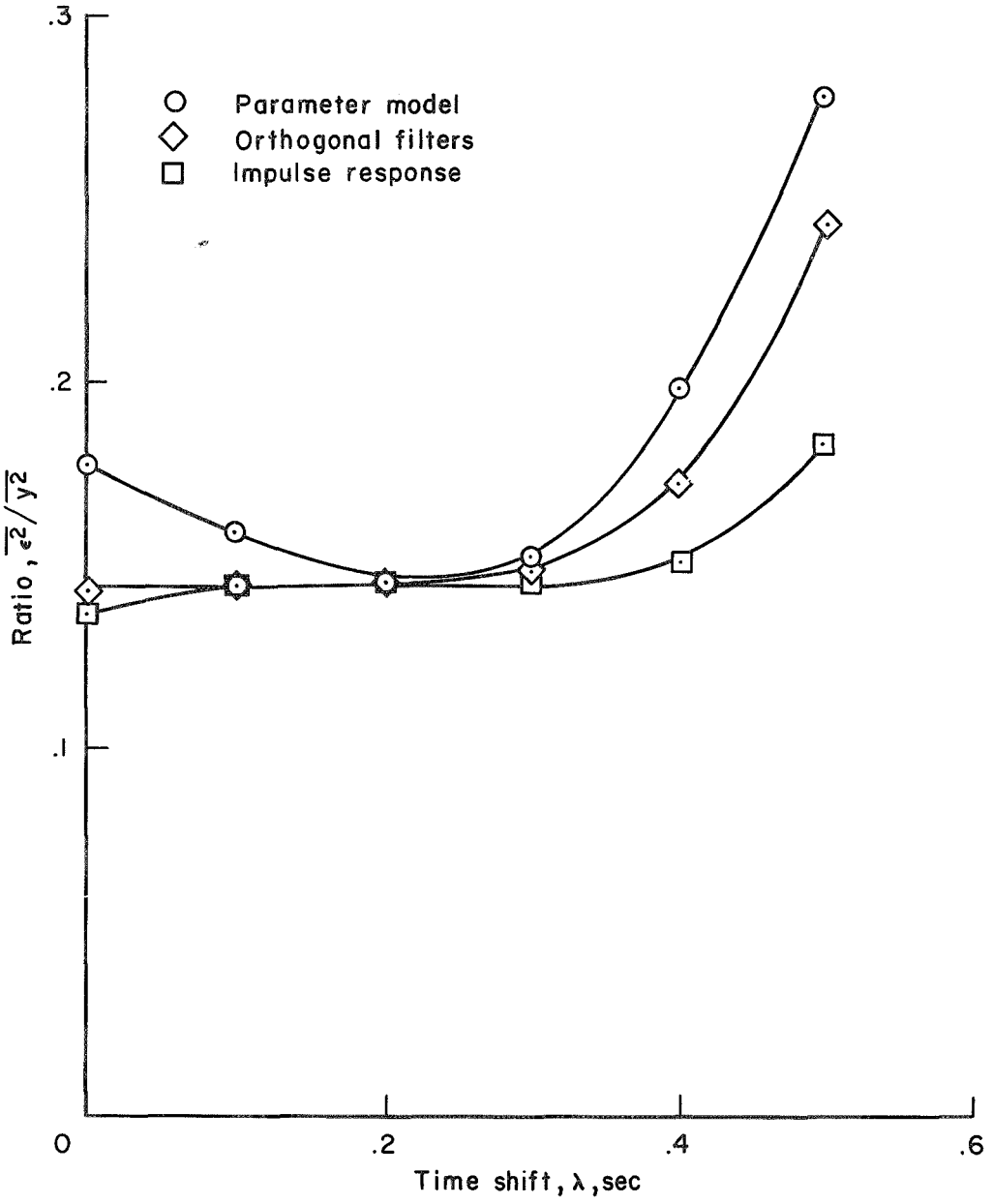

(a) Single-input task.

Figure 10.- Effect of the time shift λ on the residual.

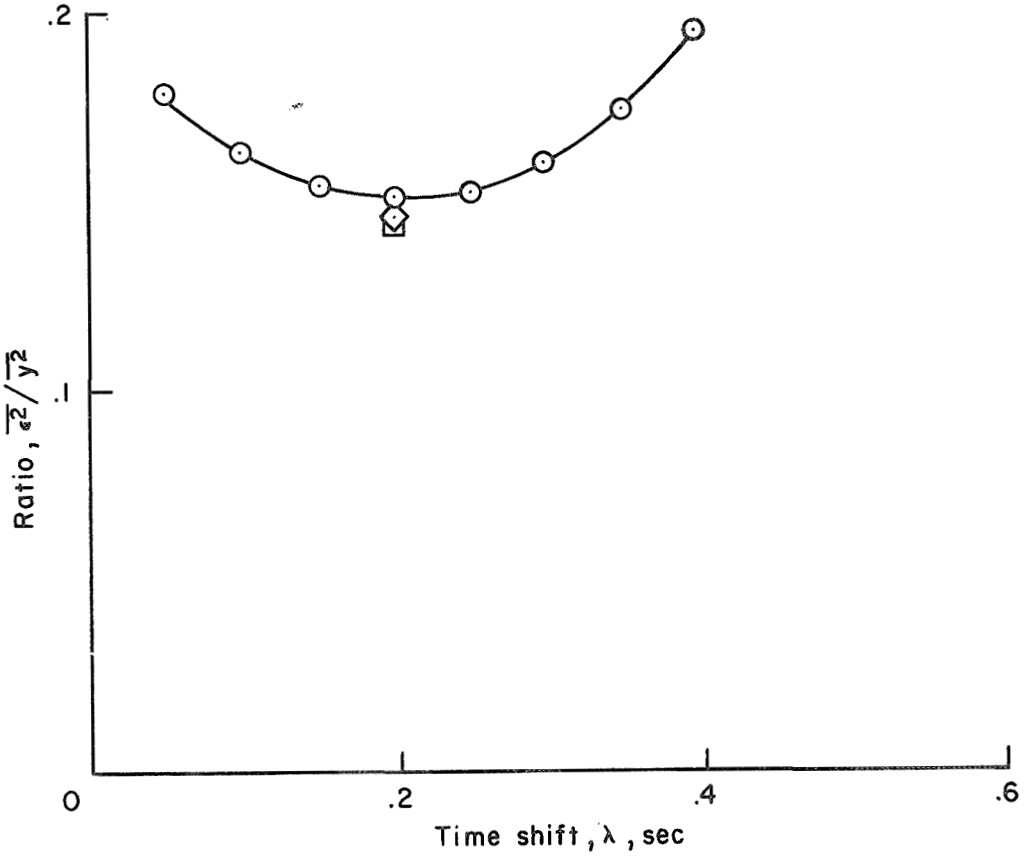

(b) Two-input task.

Figure 10.- Concluded.

NATIONAL AERONAUTICS AND SPACE ADMINISTRATION
WASHINGTON, D. C. 20546
OFFICIAL BUSINESS

FIRST CLASS MAIL

POSTAGE AND FEES PAID
NATIONAL AERONAUTICS AND
SPACE ADMINISTRATION

POSTMASTER: If Undeliverable (Section 158 Postal Manual) Do Not Return

"The aeronautical and space activities of the United States shall be conducted so as to contribute . . . to the expansion of human knowledge of phenomena in the atmosphere and space. The Administration shall provide for the widest practicable and appropriate dissemination of information concerning its activities and the results thereof."

—NATIONAL AERONAUTICS AND SPACE ACT OF 1958

NASA SCIENTIFIC AND TECHNICAL PUBLICATIONS

TECHNICAL REPORTS: Scientific and technical information considered important, complete, and a lasting contribution to existing knowledge.

TECHNICAL NOTES: Information less broad in scope but nevertheless of importance as a contribution to existing knowledge.

TECHNICAL MEMORANDUMS: Information receiving limited distribution because of preliminary data, security classification, or other reasons.

CONTRACTOR REPORTS: Scientific and technical information generated under a NASA contract or grant and considered an important contribution to existing knowledge.

TECHNICAL TRANSLATIONS: Information published in a foreign language considered to merit NASA distribution in English.

SPECIAL PUBLICATIONS: Information derived from or of value to NASA activities. Publications include conference proceedings, monographs, data compilations, handbooks, sourcebooks, and special bibliographies.

TECHNOLOGY UTILIZATION PUBLICATIONS: Information on technology used by NASA that may be of particular interest in commercial and other non-aerospace applications. Publications include Tech Briefs, Technology Utilization Reports and Technology Surveys.

Details on the availability of these publications may be obtained from:

SCIENTIFIC AND TECHNICAL INFORMATION OFFICE

NATIONAL AERONAUTICS AND SPACE ADMINISTRATION

Washington, D.C. 20546